

A WIRELESS SENSOR NETWORK
FOR MONITORING PHYSICAL ACTIVITY, PHYSIOLOGICAL RESPONSE,
AND ENVIRONMENTAL CONDITIONS

By

Michael L. Pook

A thesis
submitted in partial fulfillment
of the requirements for the degree of
Master of Science in Computer Engineering
Boise State University

May 2011

BOISE STATE UNIVERSITY GRADUATE COLLEGE

DEFENSE COMMITTEE AND FINAL READING APPROVALS

of the thesis submitted by

Michael L. Pook

Thesis Title: A Wireless Sensor Network for Monitoring Physical Activity,
Physiological Response, and Environmental Conditions

Date of Final Oral Examination: 16 March 2011

The following individuals read and discussed the thesis submitted by student Michael L. Pook, and they evaluated his presentation and response to questions during the final oral examination. They found that the student passed the final oral examination.

Sin Ming Loo, Ph.D. Chair, Supervisory Committee

R. Jacob Baker, Ph.D. Member, Supervisory Committee

Sondra M. Miller, Ph.D., P.E. Member, Supervisory Committee

The final reading approval of the thesis was granted by Sin Ming Loo, Ph.D., Chair of the Supervisory Committee. The thesis was approved for the Graduate College by John R. Pelton, Ph.D., Dean of the Graduate College.

ACKNOWLEDGMENTS

I would like to thank Dr. Sin Ming Loo for his guidance and support throughout this process and my academic career. I truly appreciate all that he has done for me as a mentor and advisor.

Additionally, I would like to thank all who were involved on the Fusion projects and this research: Ross Butler, Kelsey Drake, James Hall, Josh Kiepert, and Derek Klein.

I would like to offer special thanks to Derek Klein for his considerable assistance with the troubleshooting process and the selection of sensors. In addition, I would like to offer further thanks to Josh Kiepert for providing a substantial portion of the computer interface code and offering his technical expertise during each stage of this research.

Finally, I would like to thank my family and friends for their love and support. I am especially grateful to my parents for their support and for easing my burden in every way they could. I also appreciate Vikram Patel's assistance in testing my prototypes and generally keeping up my morale.

This work is funded by FAA Cooperative Agreement No. 04-C-ACE-BSU and 07-C-RITE-BSU¹.

¹ Although the FAA has sponsored this project, it neither endorses nor rejects the findings of this research. The presentation of this information is in the interest of invoking

ABSTRACT

A Wireless Sensor Network for Monitoring Physical Activity, Physiological Response,
and Environmental Conditions

Michael L. Pook

Master of Science in Computer Engineering

Understanding movement is an important area of research for improving comfort and safety. Data collected from accelerometers and gyros attached to multiple parts of a body can be used to determine the type of physical activity in which an individual is engaging. Correlating this data with the individual's heart rate allows for the verification of the type of activity as well as observation of the amount of physical strain experienced during the activity. Additionally, data on environmental stimuli can be gathered in order to determine their effect on physical strain. Current research in the field has been limited by both the portability and flexibility of current sensor systems. This thesis focuses on the development of a flexible wireless sensor network framework for collecting data on an individual's physical activity, the corresponding strain, and relevant environmental factors. Successful implementation of this system has been completed and results are reported.

technical community comment on the results and conclusions of the research.

TABLE OF CONTENTS

ACKNOWLEDGMENTS	iv
ABSTRACT	v
LIST OF FIGURES	ix
LIST OF ABBREVIATIONS	xi
CHAPTER 1: INTRODUCTION	1
1.1 Personal Sensor Networks	1
1.2 Physical Activity Tracking	2
1.3 Pulse Oximetry	4
1.4 Environmental Sensing	6
1.5 General Purpose Design	7
1.6 Contributions	7
1.7 Outline	8
CHAPTER 2: PREVIOUS WORK AND EXISTING TECHNOLOGY	10
2.1 Previous Research	10
2.1.1 Fusion	10
2.1.2 Micro Fusion	13
2.1.3 Firmware Design	16
2.1.4 Application to Current Research	18
2.2 Existing Technology	19
CHAPTER 3: SENSOR FRAMEWORK	26

3.1	Network Topology	28
3.2	Base and Environmental Sensor Nodes	30
3.3	Personal Sensor Nodes	31
3.4	Data Processing	32
CHAPTER 4: HARDWARE DESIGN		33
4.1	The Micro PAD	33
4.2	Biomedical System Design	35
4.2.1	Prototype 1: Pulse Oximeter	36
4.2.2	Prototype 2: PIP 4000	40
4.2.3	Prototype 3: MiFOXI	42
4.3	Environmental Sensor Daughterboards	45
CHAPTER 5: SOFTWARE DESIGN		48
5.1	Micro PAD Firmware	48
5.2	Biomedical System Firmware	50
5.2.1	LED Control	51
5.2.2	DC Tracking	53
5.2.3	Signal Filtering	55
5.2.4	Peak Detection	58
5.2.5	Pulse and SpO ₂ Calculation	60
5.3	Environmental Sensor Firmware	61
5.4	Computer Software	62
5.4.1	BSU Sensor Graphing Utility	63
5.4.2	BSU Sensor Monitor Lite Program	64

CHAPTER 6: RESULTS	66
6.1 Micro PAD	66
6.1.1 Test 1 Analysis	69
6.1.2 Test 2 Analysis	71
6.1.3 Test 3 Analysis	77
6.2 Pulse Oximeter	80
6.3 Environmental Sensor Daughterboards	85
CHAPTER 7: CONCLUSIONS AND FUTURE WORK	88
7.1 Personal Sensor Network	88
7.2 Micro PAD	89
7.3 Biomedical System	90
7.4 Environmental Sensing	92
7.5 General Purpose Design	92
REFERENCES	94

LIST OF FIGURES

Figure 2.1	The Fusion (6.85 x 9.5 cm)	11
Figure 2.2	The Micro Fusion (3.83 x 8.10 cm)	14
Figure 2.3	Code Layering Diagram Depicting High and Low Level Layers with Multiple Subdivisions and Code Module Examples for Each Layer	16
Figure 3.1	Node Placement on Test Subject in Sitting and Standing Positions with Nodes on the Chest, Arm, and Upper Leg	26
Figure 3.2	Mesh and Star Network Topologies	29
Figure 4.1	Micro PAD (3.93 x 6.33 cm)	34
Figure 4.2	Micro PAD Axis Orientations	35
Figure 4.3	Pulse Oximeter Prototype (1.63 x 3.4 cm)	37
Figure 4.4	Pulse Oximeter Transmit (TX) Schematic	38
Figure 4.5	Pulse Oximeter Receive (RX) Schematic	39
Figure 4.6	The PIP 4000 (7.14 x 4.64 cm)	41
Figure 4.7	The MiFOXI (5.08 x 6.79 cm)	44
Figure 4.8	MiFOXI Daughter (6.93 x 4.27 cm)	45
Figure 4.9	Environmental Sensor Daughterboards	46
Figure 5.1	Fusion Network Data Format Strings	49
Figure 5.2	Pulse Oximeter Firmware Block Diagram Showing Hardware (Red Outline) and Software (Black Outline) Blocks	50
Figure 5.3	Spectral Responsivity of the Photodiode [24]	52
Figure 5.4	DC Tracking Filter Design and Performance Figures	54
Figure 5.5	Heartbeat Signal Before Digital Filtering	56
Figure 5.6	Butterworth Second Order Filter Block Diagram	57
Figure 5.7	Digital LPF Magnitude Response and Filtered Heartbeat Signal	58
Figure 5.8	BSU Sensor Graphing Utility Screenshot	64

Figure 5.9	BSU Sensor Monitor Lite Program Screenshot	65
Figure 6.1	Micro PAD Node Placements and Sensor Axis Orientations	67
Figure 6.2	Test 1 Complete Activity Results for the Chest Accelerometer	68
Figure 6.3	Test 1 Sit, Stand, Bend, and Walk Results for the Chest Accelerometer	70
Figure 6.4	Test 1 Walk and Run Results for the Chest Accelerometer.....	71
Figure 6.5	Test 2 Run and Spin Results for Chest Gyroscope and Accelerometer	73
Figure 6.6	Test 2 Stationary Activity Results for Chest, Arm, and Leg Accelerometers	77
Figure 6.7	Test 3 Data for Unknown Activities Performed by Test Subject	79
Figure 6.8	SpO ₂ and Pulse Data Displayed on a HyperTerminal	81
Figure 6.9	First Rest Activity Data for Accelerometers and Pulse Oximeter	83
Figure 6.10	Running Activity Data for Chest Accelerometer and Pulse Oximeter	84
Figure 6.11	Second Rest Activity Data for Accelerometers and Pulse Oximeter	85
Figure 6.12	Environmental Sensor Data	87
Figure 7.1	Redesigned Oximeter Receive Circuit	92

LIST OF ABBREVIATIONS

AC	Alternating Current
ADC	Analog-to-Digital Converter
BPM	Beats Per Minute
BSU	Boise State University
CO	Carbon Monoxide
CO ₂	Carbon Dioxide
cm	Centimeter
CSV	Comma Separated Values
CON	Carbon Monoxide, Oxygen, and Ammonia
DAC	Digital-to-Analog Converter
DSP	Digital Signal Processor/Processing
DC	Direct Current
DMA	Direct Memory Access
ECG	Electrocardiogram
GPIO	General Purpose Input/Output
HuT	Humidity and Temperature
ID	Identification
IIR	Infinite Impulse Response
IR	Infrared
I/O	Input/Output
I ² C	Inter-Integrated Circuit
ISR	Interrupt Service Routine
LED	Light Emitting Diode
LPF	Low Pass Filter
NH ₃	Ammonia
MiFOXI	Micro Fusion Oximeter rev I
mm	Millimeter
mV	Millivolt
PDA	Personal Digital Assistant
PIP	Personal Information Processor
PAD	Physical Activity Daughterboard
PWM	Pulse Width Modulation
PCB	Printed Circuit Board

RF	Radio Frequency
RAM	Random Access Memory
RX	Receive
SpO ₂	Saturation of Peripheral Oxygen
SD	Secure Digital
SPI	Serial Peripheral Interface
TI	Texas Instruments
TX	Transmit
USB	Universal Serial Bus
UART	Universal Asynchronous Receiver/Transmitter
WPSN	Wireless Personal Sensor Network

CHAPTER 1: INTRODUCTION

1.1 Personal Sensor Networks

As technology evolves, the world around us changes, and we find ourselves engaging in new activities in varying environments. Advancements in the twentieth century saw mankind flying in aircraft (an enclosed and confined environment), playing new sports on synthetic fields while using specialized equipment (both indoors and outdoors), and working in large buildings (a ventilated indoor environment) with electronically controlled environments. Understanding these new environments and the effect they have on people has been, and continues to be, an important part of improving safety and comfort. Sensor networks are a valuable tool for accomplishing such a task.

In general, sensor networks are comprised of multiple nodes collecting data in different locations. The nodes are embedded systems with each having its own microcontroller, sensors, and a means of communication with the rest of the network and outside world. Personal sensor networks are worn by an individual to monitor movement and physiological characteristics (e.g., heart rate, blood oxygenation, respiration, etc.) at different parts of the body. Initially, communications for such systems were handled via wired connections between each node and any external systems. Although this is still the case for many systems, advancements in the field of wireless communications have caused a surge in the number of wireless sensing solutions. Wireless personal sensor networks (WPSN) have two very important benefits. First, the lack of wires between

nodes allows the test subject to have full range of motion. Second, WPSN's do not have to be tethered to external interfaces (e.g., display terminals or computers). This gives them the ability to be used outside controlled laboratory environments. One key downside to the use of WPSN's is the perception of health risks associated with wireless technology. Many concerns have been raised about RF exposure causing cancer and other various problems. However, studies conducted to determine the validity of these concerns have found no evidence to support such claims for commercially available wireless networks [1].

This thesis focuses on the development of a general purpose WPSN framework for tracking physical activity, physical strain, and environmental conditions. It includes the design of a flexible sensor network capable of adapting to multiple situations and expanding to include different physical and environmental sensors as needed. The system further includes the design of a computer interface for real-time and post collection data processing.

1.2 Physical Activity Tracking

Physical activity tracking involves monitoring motion of different parts of the body and the strain associated with various tasks. This research leads to a better understanding of general human motion and physiological response. Such knowledge allows for the advancement of ergonomics, safety equipment, and safety training in a wide variety of occupational and recreational activities. Although useful in preventing injuries and improving athletic performance, advancements in this field can also be used for various applications ranging from predicting and preventing injuries in rescue

workers to improving ergonomics in offices and transportation vehicles (e.g., airplanes, busses, cars, etc.) [2].

Due to its importance to a wide range of applications, scientists have put decades of research into the study of human movement and the associated physical strain. As early as 1960, studies were being conducted to relate vertical trunk movement of an individual to their energy expenditure. By 1978, single axis accelerometers were being used to track movement for similar studies. Then, the beginning of the 90's saw the widespread use of both uniaxial and triaxial accelerometers in laboratory studies of physical activity tracking as well as personal use by professional and amateur athletes [3].

Physical activity tracking can be done using a variety of methods and technologies. Prototype devices have been developed utilizing a myriad of sensors including accelerometers, gyroscopes, digital compasses, cameras, pulse oximeters, and electrocardiogram (ECG) sensors. The most prevalent of these technologies is the accelerometer based system. The basic principle is to use accelerometer nodes placed at key points of interest on the body to monitor their acceleration individually and with respect to one another. This data can then be processed to determine the type and extent of motion. In order to improve the quality of the data, more sensors can be included in the accelerometer nodes. For instance, gyroscopes can be used to measure angular acceleration in order to track rotational motion of the arms, legs, and head. Another option is to include a sensor capable of measuring heart rate (e.g., pulse oximeter, ECG, etc.) to help in the determination physical strain. This thesis will focus on the creation of a system capable of utilizing any relevant sensor input, but the initial set includes

accelerometers, gyroscopes, a platform for recording data from environmental sensors (e.g., CO₂, temperature, humidity, etc.), and a pulse oximeter.

1.3 Pulse Oximetry

Metabolism of oxygen is necessary to sustain life, and lower oxygenation of arterial blood means less oxygen available for metabolism. Oxygenation of less than 90% in arterial blood is known as hypoxemia and can result in a number of conditions ranging from shortness of breath to death if left untreated. Thus, as an essential component of human survival, oxygenation can be a useful tool in determining a person's well being [4] [5].

Pulse oximetry as it is known today was first developed in 1972 by Takuo Aoyagi as a non-invasive means of measuring O₂ saturation (oxygenation) of hemoglobin in arterial blood of hospital patients [6]. The majority of current pulse oximeters measure saturation of peripheral oxygen (SpO₂). The basic method used by a pulse oximeter to measure SpO₂ involves using a photodetector to measure the attenuation of light from two light sources as it passes through a person's tissue (usually on the finger or ear). One light source emits light with an 800-940 nm wavelength (infrared, IR). The other source produces light with a 600-700 nm wavelength (red). The IR light is absorbed by oxygenated hemoglobin, and the red light is absorbed by the deoxygenated hemoglobin. Each time the heart beats, blood flow increases and causes an increase in the current produced by the photodetector. This increase is detected and the peak value for each source is measured. Additionally, the occurrence of such a peak is used to calculate the pulse rate. Once the intensity of light that passes through the tissue is measured for each source, the Beer-Lambert Law (see Equation 1) is used to determine the SpO₂ [7, 8]:

$$I = I_0 e^{-(\alpha(\lambda)cd)} \quad (1)$$

In Equation 1, I is the intensity of light that comes out from the medium, I_0 is the intensity of incident light that enters the medium, $\alpha(\lambda)$ is a wavelength-dependent absorbance coefficient, d is the path length through the medium, and c is the analyte concentration [7].

Measurement of SpO₂ using a pulse oximeter is not exact and can only provide an approximation of arterial blood oxygenation. As compared to the most accurate method for calculating SpO₂ (CO-oximetry via blood analyses done in a laboratory), pulse oximetry readings are within $\pm(2-4)\%$ of the actual SpO₂ value at best [9]. Furthermore, oximeter readings can become skewed by several factors including anemia, carbon monoxide poisoning, cold extremities (where the sensor is applied), and movement (e.g., shaking, or shivering). This makes the measurement less reliable than other methods (e.g., those involving blood analyses in a laboratory) [10]. However, for instances where blood analysis is not an option and approximation will suffice, the ability of pulse oximetry to provide a good approximation via non-invasive methods makes it a very good option.

The heart rate data collected from the pulse oximeter could be used for a number of applications. For general physical activity tracking, the data from the pulse calculation can be used to determine the intensity of a subject's physical strain during varying activities. Increased physical activity causes an increase in heart rate. A more strenuous cardiovascular exercise (e.g., running, aerobics, etc.) will result in a faster pulse. Thus, increased heart rates can be used as an indicator of increased physical strain. When

correlated with a lack of physical activity, an increased heart rate could be used to detect possible health problems (e.g., heart attack, onset of pain, etc.) as in the research conducted in [2]. It should be noted that physical strain is not limited to cardiovascular response. For example, weight lifting may not increase a person's heart rate as much as running a mile, but lifting heavy objects repeatedly is still a strenuous activity. Another biomedical sensor may be required to measure physical strain with respect to this and similar activities.

The SpO₂ measurement from the pulse oximeter can also be useful in multiple ways. Physical activity requires an increased intake and use of oxygen. Low SpO₂ levels during active periods can be indicative of pulmonary health problems (e.g., chronic obstructive pulmonary disorder) [11]. Also, according to a study conducted at Johns Hopkins, low arterial blood oxygenation during exercise could be indicative of heart problems [12]. Studies conducted related to the research of such diseases require a system capable of recoding physical activity data and SpO₂ levels simultaneously.

1.4 Environmental Sensing

The effect of environmental conditions on a person's well-being and comfort is an important area of research. Many studies have been conducted in this area to find these effects and to monitor relevant conditions for the purpose of improving comfort and safety. The results of these studies have provided researchers with a wealth of information on physiological responses to environmental stimuli. This knowledge can be applied directly to many areas of physical activity tracking to greatly improve the quality and interpretation of data. As mentioned in Section 1.3, a low SpO₂ level recorded during exercise could indicate a health problem. However, environmental factors can also

contribute to this reading. For example, suppose a test subject is running on a treadmill inside a lab, and an ventilation failure causes the room's carbon dioxide level to exceed 2000 ppm. Although a pre-existing health problem could still possibly explain their low blood oxygenation, a more probable explanation is the lack of breathable O₂ due to the rise in CO₂. By including environmental conditions (e.g., CO, CO₂, temperature, etc.) in the analysis of physical activity tracking, a researcher is able to gain a more complete picture of what their data means.

1.5 General Purpose Design

In order to design a flexible sensor system, special consideration must be given to both hardware and firmware development. The goal of a flexible system is to be able to incorporate new sensors and functionality with minimal firmware changes and without any redesign of hardware. The hardware has to be designed to supply commonly used voltages, communicate via standard protocols, and have a wireless radio capable of managing reasonably high data throughput and network communications. The firmware needs to be modular and properly layered. Keeping drivers for generic system tasks (e.g., scheduling, ADC measurements, data storage, etc.) and communication protocols separate from sensor specific functions results in a system that is highly reconfigurable and easily expandable.

1.6 Contributions

The key contribution of this work is the development of a general-purpose framework for physical activity tracking via a WPSN. Many researchers have developed similar systems for targeted applications (see Section 2.2). While these systems are fixed in the number and type of sensors, the current work focuses on system flexibility. The

system created for this thesis has been designed such that it can incorporate a variety of sensors with minimal hardware and firmware additions. New sensors can be added, and the system can be reconfigured without the need for lengthy development time.

Additionally, few existing technologies incorporate both biomedical and environmental sensor technologies to explore physiological response to environmental and physical activity stimuli. Thus, the system designed for the current work utilizes both sensor types in order improve its ability to be used in a multitude of experimental applications.

Furthermore, many of the existing technologies choose either data logging or real-time processing of data. This limits the ability of the systems to adapt to the needs of researchers conducting experiments in situations requiring the opposite type of data processing or both types. As an answer to this particular problem, the current system designed for this thesis includes real-time processing and data logging with post-experiment processing capabilities in order to adapt to the needs of different situations.

The goal of this research has been to design a WPSN framework with the highest possible flexibility in order to adapt for use in the widest range of physical activity tracking applications.

1.7 Outline

The following chapters discuss the topics surrounding physical activity monitoring, environmental monitoring, and physiological response as they relate to the scope of this thesis. Chapter 2 discusses the work done prior to the start of the thesis including descriptions of the environmental sensor node and the physical activity system motherboard designs. Additionally, the second section in Chapter 2 contains a description of existing technology developed by other researchers. Chapter 3 covers the

implementation of the wireless sensor network architecture. A detail of the hardware design for the accelerometer/gyro sensor nodes and wireless pulse oximeter node can be found in Chapter 4. The discussion of the software design in Chapter 5 details both the firmware development for the sensor nodes and the computer interface software. The results of the designs are detailed in Chapter 6. Finally, Chapter 7 offers conclusions and a discussion of future work.

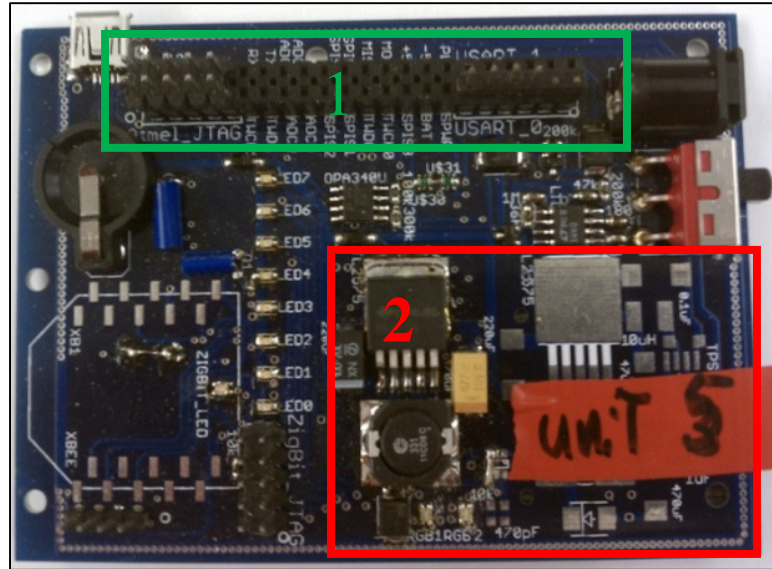
CHAPTER 2: PREVIOUS WORK AND EXISTING TECHNOLOGY

2.1 Previous Research

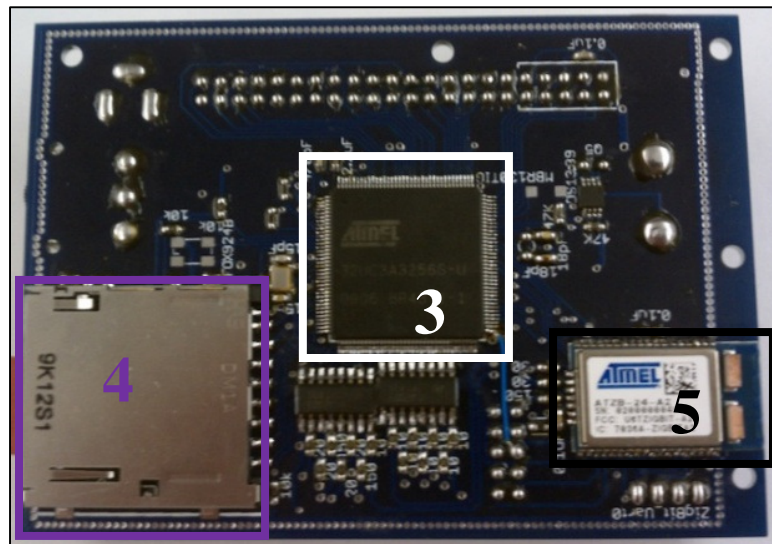
The key design aspect for any flexible sensor system is the motherboard. In order to be capable of accepting a wide range of sensors and adapting to meet the changing needs of researchers, a motherboard must be designed such that it can provide ample resources (e.g., communications interfaces, voltage levels, data storage, etc.) for a diverse sensor set. Additionally, physical size and power consumption must also be considered in order to allow for use of the sensor system in various situations. Finally, a design must include a method for transmitting or recording data. The current research includes two such designs: the Fusion and Micro Fusion.

2.1.1 Fusion

The Fusion was designed for the Hartman Systems Integration Laboratory research on air quality in airliner cabins. The focus of the design was the creation of a flexible system capable of the high data throughput necessary for the use of sensor data fusion algorithms. As such, power consumption and board size were secondary concerns. The final design is shown in Figure 2.1.



(a) Top



(b) Bottom

Figure 2.1: The Fusion (6.85 x 9.5 cm)

- (1) Breakout Header; (2) Power Supplies; (3) Microcontroller; (4) SD Card Holder;**
(5) Zigbit Radio

The Fusion was designed in such a way as to allow for future expansion via the use of daughterboards with an unknown set of requirements. In order to provide the resources needed for various sensor types, a microcontroller had to be selected that could

run at high speeds, handle various communication protocols, offer a selection of peripheral devices, and supply enough memory to allow for a large codebase. Given a system with a large number of sensors needing to be read every few hundredths of a second, the microcontroller would need to operate fast enough to run the code for each sensor and contain enough memory to store and execute the code. Thus, in order to achieve the greatest level of flexibility, higher speeds and more memory were essential. The necessary peripheral devices were more difficult to determine. Given an unknown number of sensors and limited knowledge of possible future applications for the Fusion, knowing all of the peripheral devices that could be useful was impossible. However, devices such as ADC's, DAC's, general purpose input/output (GPIO) pins, and direct memory access (DMA) controllers are commonly needed for many sensors. Useful communications protocols were far simpler to determine. The requirement for this factor was to find a microcontroller with at least one dedicated port for each of the major protocols (e.g., I²C, SPI, UART, and USB) and multiple ports for the most commonly used protocols. After all of the above factors were taken into consideration, the final choice was Atmel's 32-bit ATUC3A3256S.

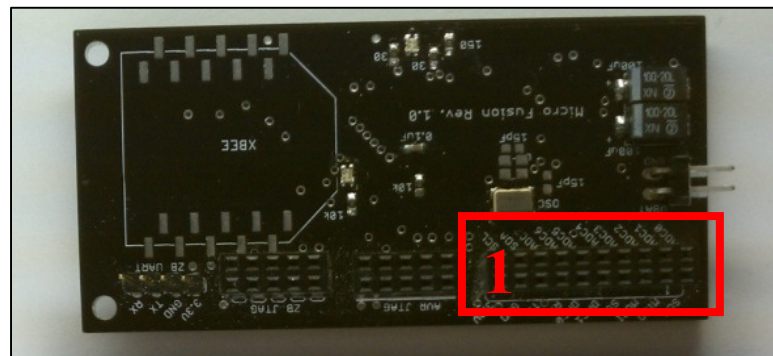
Although the microcontroller is an important component in the design of a motherboard, other devices also contribute to the flexibility of a system. The available voltage levels can be a limiting factor for the sensors that can be integrated into a system. Regulators can be built into the design of daughterboards to meet sensor specific needs, but the inclusion of regulators on the motherboard, other than those required for the microcontroller, simplify the design of daughterboards and keep their designs smaller. For these reasons, the Fusion includes voltage regulators for 3.3V, 5V, and -5V.

Although these are not the only voltages used by sensors, they are the most common. In addition to the various power supply abilities, the Fusion also has two wireless radio options (Atmel's Zigbit and Digi's XBee) for communicating via the Zigbee protocol. Either device will allow the Fusion to form mesh networks for transmitting data between sensor nodes. The Xbee provides the researcher with a simple interface for data transmission (via UART) while the Zigbit allows for a much higher data throughput (via SPI). While communication between nodes in a wireless network is important, delivering data to the researcher is also key. The Fusion has two solutions for this as well. Data can either be stored to the onboard SD card for post experiment analysis or streamed via UART or UART controlled wireless radio (e.g., Bluetooth, WiFi, etc.) to a computer for real-time analysis. Figure 2.1 (a) also depicts a USB port. This could be used as another method for transferring data to the researcher, but the necessary firmware has yet to be added. For data to be meaningful, many applications require knowledge of precisely when the measurements took place. To this end, the design includes a real-time clock external to the microcontroller and powered by its own coin cell battery. This allows the date and time to be set and kept accurate even when the system is not being powered.

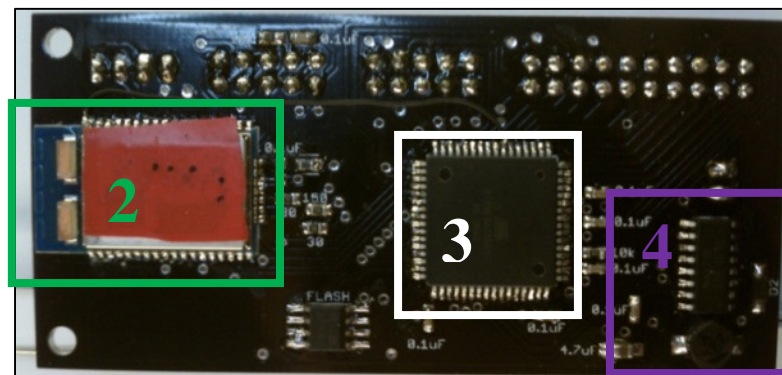
2.1.2 Micro Fusion

The Micro Fusion was also designed by the Hartman Systems Integration Laboratory for their research in airliner cabin air quality. This design, however, had a different set of priorities. As previously described, the Fusion was designed as their network's Clydesdale. That device has all of the processing power and data throughput capabilities necessary to handle any given task. However, as shown in Figure 2.1, the Fusion is rather large (6.85x9.5cm) and has a lot more hardware for functionality that

simpler tasks will never need. Furthermore, even though its design took power consumption into consideration, it draws more current than should be necessary for an application involving one or two sensors per node. For these reasons, the Micro Fusion was created as a smaller (3.83x8.10cm), low power version of the Fusion with a more limited feature set. Figure 2.2 depicts the Micro Fusion design.



(a) Top



(b) Bottom

Figure 2.2: The Micro Fusion (3.83 x 8.10 cm)

(1) Breakout Header; (2) Zigbit Radio; (3) Microcontroller; (4) Power Supply

Although it lacks some of the features that make the Fusion flexible, the Micro Fusion is by no means a rigid design. The abilities to adapt to the changing needs of researchers and reconfigure to include a diverse sensor set were still important

considerations during the design process. The selection of the microcontroller was still subjected to the same set of requirements as the previous design. The key difference between the two selections was the greater emphasis on power consumption and physical chip size used to select the microcontroller for the Micro Fusion. The 8-bit ATXMEGA256A3 chosen for the final design still has the common communication protocols, requisite peripheral devices, high speed capabilities, and adequate memory capacity to make the Micro Fusion a flexible motherboard. It just has fewer ports/peripherals, lower speeds, and less memory than its 32 bit counterpart on the Fusion. This makes the Micro Fusion a less flexible option in terms of the number of sensors and amount of data throughput it can handle but also makes the device more suitable for applications involving few sensors, requiring small size, and needing low power consumption (e.g., physical motion tracking).

The requirement for a small board size made elimination of some additional functionality necessary, but the Micro Fusion still has a few devices external to its microcontroller. The first devices cut from this design were the extra voltage regulators. The Micro Fusion has only the 3.3V regulator. As previously discussed for the Fusion hardware, given that this design was made to be expanded via the use of daughterboards, eliminating the extra power supplies does not necessarily exclude sensors with different power requirements. It just translates into more circuitry on the daughterboards for those particular sensors. Since 3.3V is the most commonly used supply by sensors and it could be used to power the microcontroller, it was selected as the only regulator to remain on the design. Similarly to the Fusion, this design includes a wireless radio for transmitting data between sensor nodes. Excluding the option to use Digi's XBee radio in favor of

Atmel's Zigbit kept the design smaller and removed the possibility for a data throughput bottleneck that could have been created by UART communication between the microcontroller and the radio. For transferring data to the researcher, the Micro Fusion uses UART communication either directly through a computer's RS232 port or via a UART controlled wireless radio as its primary method. This design does not include an SD card for storage. Instead, a 2MB flash chip was added to the Micro Fusion. Using a piece of flash memory in a small footprint IC instead of an SD card allowed for external data storage and made the board design smaller.

2.1.3 Firmware Design

The flexible hardware on a motherboard is only half of the design. True flexibility requires the motherboard to have a good firmware design as well. The firmware for both motherboards was written to have high cohesion, low coupling, and a well defined hierarchy. In other words, the code is split into multiple layers each with its own set of independent modules with well defined tasks in order to promote greater portability and flexibility (see Figure 2.3) [13].

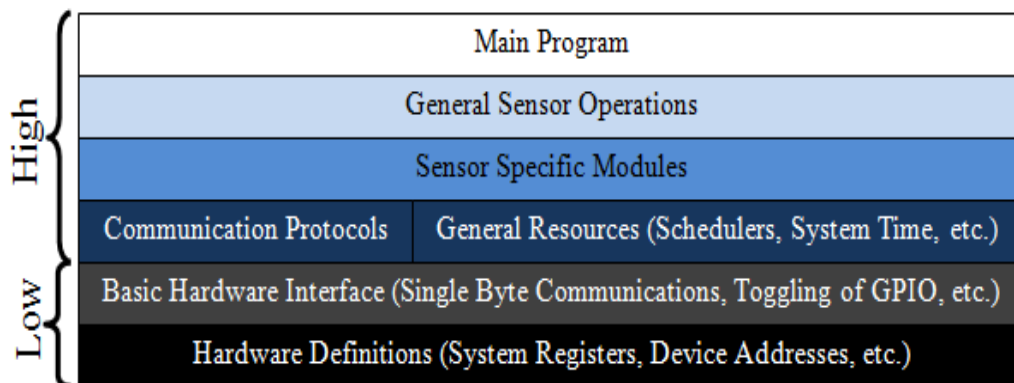


Figure 2.3: Code Layering Diagram Depicting High and Low Level Layers with Multiple Subdivisions and Code Module Examples for Each Layer

Putting the code into task specific modules eliminates the need for redundant programming and speeds up the development process. For example, both sets of firmware include independent modules for each communication protocol. This means that the sensor specific interface code of multiple sensors sharing a common protocol can all use the functions defined in their protocol's module to communicate with their hardware. This same principle is applied throughout the code for every resource from GPIO pin and ADC controls to the system scheduler and data transmission services. Thus, the addition of new sensors is simplified, because code for controlling all system resources has been previously written.

The modularity of the code makes it flexible for adding new sensors to the existing hardware, but another important consideration is the ability to move the sensors and their code to another type of hardware. Layering is a key factor in determining portability. The majority of the code written for the Fusion hardware was ported to the Micro Fusion, and a fair amount of the useful pieces of code generated for the Micro Fusion project was ported back to the Fusion hardware. Although both devices use Atmel microcontrollers, the devices are from separate families with vastly different architectures. Proper layering of the code (in conjunction with few other good coding practices [13]) made this feat possible. The firmware can be split into two main layers each with their own set of subdivisions: high level and low level code (see Figure 2.3). As defined by Pook et al., the low level code comprises all the functions that handle communication to the actual hardware [13]. This code has knowledge of all the registers in the microcontroller and handles bit level operations. The high level code encompasses all functionality that runs the main tasks of the system. High level tasks include such

functions as scheduling sensor measurements, writing data to the SD card, and using the communication protocols to send data to devices external to the microcontroller.

Although this layer makes calls to the low level code, it has no knowledge of the hardware. Due to this definitive separation between the high and low level functionality, the main system operations (high level) can be moved from one piece of hardware to another with relative ease. All that is required is a re-write of the hardware interface (low level) [13]. Thus, although the hardware was designed to adapt as researchers needs dictated, the high level firmware could continue to be useful in the event that advances in technology made a hardware revision advantageous.

2.1.4 Application to Current Research

As stated in the introduction to Section 2.1, the current research uses both the Fusion and Micro Fusion motherboards for the physical activity tracking network. Given the capabilities and flexibility of the Fusion design, it could be argued that it alone would be sufficient for the goals of this thesis. However, the size of the design could make it less comfortable for a test subject to wear. The Micro Fusion's smaller size makes it better suited to being attached to a person's body. Additionally, its lower power consumption translates into fewer batteries that have to be worn for the same given system run-time. The Micro Fusion, however, is not perfectly suited for every necessary task in the network. For very simple applications involving few nodes, the Micro Fusion may work as a base node for collecting and routing data from the network. Given an application with multiple test subjects and a large number of nodes/sensors, the Micro Fusion will most likely be unable to handle the required data throughput. Thus, the Fusion is required as a base node to handle the possibility of high data throughput in

order to ensure that vital data is not lost. So, although arguments could be made for using just one of the two motherboards, employing both devices improves the flexibility of the network.

2.2 Existing Technology

As previously stated, the widespread applications of physical activity tracking have made it a very important area of research. As such, several groups have completed work on various hardware prototypes for collecting and processing data. Although these devices have performed well for their targeted applications [2, 3, 14-21], few have made strides towards a flexible system capable of taking all factors affecting physical activity and physiological response into consideration. However, since their work relates closely to the goals of this thesis, a comparison of the current research to theirs is important.

Wixted et al. [3], Khan et al. [14], and Bouten et al. [15] conducted research associating the accelerometer data to physical strain, but none of the systems utilized a WPSN, tracked environmental or biomedical factors, nor took full advantage of wireless communications for data transmission and processing. The systems designed for the research completed in [3] through [14] provide the most basic features for physical activity monitoring. The primary focus for the research teams was the detection of movement. To this end, all three systems used a single triaxial accelerometer mounted to the torso of an individual to measure movement. This allowed the groups to measure a person's displacement and make such determinations as to whether the individual was walking, running, or at rest. Additionally, the researchers of [14] claim that their algorithms are capable of distinguishing between 15 different types of displacement related activities including the previously mentioned activities, movement on an inclined

plane, and transitional activities (e.g., moving between laying down and standing, etc.). Although this works well for certain activities, the shortcomings of such a system for widespread applications are readily apparent. As stated in their own assessments of the designs, the system is ineffective for measuring physical activity for stationary exercises (e.g., weight lifting, stationary aerobics, etc.) [3] [15]. Using multiple accelerometers connected to different parts of the body would have allowed the systems to monitor such activities. Another area where these systems fail for general use is in the diversity of their sensor sets. Determining the strain induced from an activity requires that other factors capable of affecting physiological response be accounted for and removed from the statistical analysis. Thus, a system that cannot measure environmental stimuli or record biomedical data is incapable of checking physiological response and verifying physical strain given a wide range of situations and environmental conditions. The final way in which these systems fall short of being useful for a wide range of applications is their method of data collection. The system of [3] utilizes IR communication to transmit data to a computer interface. Thus, it not only requires a computer to be useful but also must have line-of-sight communication with said interface. This greatly reduces the mobility and, consequently, the usefulness of the system for general purpose applications. The systems described in [14] and [15] are only capable of logging data for post-experiment processing. Although this is adequate for many applications, some experiments require the ability to process data in real-time.

The systems developed for the research conducted in [16] through [18] made significant improvements as compared to the designs previously discussed. First, these systems use WPSN's to track motion instead of a single sensor node. Thus, they are

capable of measuring stationary exertion as well as activities involving more displacement of an individual (e.g., running, walking, etc.). Second, although both devices still focus on using accelerometers, the system described in [17] and [18] also includes digital compasses to record the direction of displacement. The addition of an extra sensor type improves the range of applications for the system. However, although motion tracking is a vital component, physical activity tracking for a wide range of applications requires a more diverse sensor set (e.g., environmental and biomedical sensors). Thus, both of these designs still share this shortcoming with those from [3, 14, 15]. Furthermore, similarly to the design in [3], the designs from [16] through [18] rely exclusively real-time data processing. Although they improved upon the idea of transmitting data by using wireless radios that do not require line-of-sight (as opposed to the IR communication of [3]), this still poses a problem for experiments where wireless transmission to a computer is impractical.

Parkka et al. [19] also designed a measurement system with considerable advantages over the systems described in [3, 14, 15]. The design of [19] does not use a WPSN, but it is still capable of recognizing stationary exertion. In order to achieve this capability, the system uses three identical data logging devices placed on the ankle, waist, and wrist of the test subject. This allows researchers to monitor the different limbs and trunk movement. However, this solution does not allow for the collection of data in a single location. Data must be collected individually by each node and merged/organized before processing and analysis can occur. In a WPSN system, the data can be recorded into a single location in order to simplify data processing and analysis. Furthermore, the system clocks must be synchronized on each device before an experiment in order to

provide a means of correlating the data recorded by all three units. If the design used a WPSN, the synchronization process could be automated by the network. This would reduce the chance of timestamp errors and simplify the data collection process. Similar to the inclusion of compasses in [17] and [18] to improve motion tracking abilities, the design of [19] incorporates gyroscopes into its sensor nodes. This allows it to better discern rotational movement and improves its range of suitable applications. However, this design still excludes other valuable sensors (e.g., biomedical and environmental). Furthermore, the lack of real-time processing capabilities is another point where this design is lacking. Thus, although [19] has an interesting solution to tracking stationary activity, it still does not include the features necessary to make it a viable option for physical activity tracking over a wide range of situations.

Of the systems discussed thus far, the one developed in [20] has the most complete feature set. It combines the necessary WPSN capabilities, motion tracking, and biomedical aspects into a single package. The key technology of this design is no different from the systems of [16] through [18]. Triaxial accelerometers are still used in a WPSN to track physical activity, but an ECG sensor is included in order to verify activity by associating increased heart rates with increased physical strain. Based on the outcomes of their study, the authors of [20] arrived at the conclusion that heart rate provided minimal improvement to the results of their algorithms. However, it should be noted that other researchers determined that heart rate provided significant improvements in their physical activity tracking application and found it useful for determining dangerous conditions (e.g., high heart rate while at rest with no previous physical exertion) [2]. Thus, although the addition of the heart rate monitor was useless for their research, the

design from [20] still improved its range of useful applications with its added sensing capabilities. However, the system created by Tapia et al. [20] still excluded environmental factors and relied solely on real-time processing via wireless transmission of data. Given an application where use of a computer system is impractical, the system in [20] has no means of data logging.

Chuo et al. [21] conducted some very interesting research on physical activity and vitals monitoring. For their hardware, they chose to forgo using a WPSN and focused instead on a single multi-sensor node. By employing the same methods discussed in [3] and [15], they were able to use a single triaxial accelerometer to discern various movements and physical activities. Their system also incorporated a thermistor for detecting body temperature and ECG circuitry for measuring heart rate. For data processing, their system communicates with a cell phone or PDA via a Zigbee to Bluetooth bridge. The system cannot log data without a phone (or Bluetooth enabled device). However, a phone or PDA is easy enough to carry during experiments. The entire setup (excluding the cell phone) was manufactured on a flexible printed circuit board (PCB) that folds into a compact shape and attaches directly to a person's sternum. Thus, they are able to monitor basic physical activity and the associated physiological response using minimum hardware in a compact system [21]. Although their design is incredibly useful for their given applications, the system is not without its downsides. Due to its miniaturized design, the system is incapable of easy expansion to include more and newer sensors. Furthermore, the system excludes environmental sensors and, as previously mentioned, does not include WPSN support. Multiple nodes would give a

more accurate interpretation of motion, and environmental sensors would give a complete view of all factors affecting physiological response.

The ProeTEX device developed for the research completed in [2] would work very well for a myriad of situations. The system uses circuitry woven directly into garments worn by test subjects. Because the WPSN is woven directly into garments, placement of the sensors at correct locations is eliminated as a source of error. The sensors include accelerometers, an ECG sensor, environmental temperature sensor, and toxic gas sensors that wirelessly communicate to a computer interface. This design seems capable of monitoring most of the factors associated with physical activity tracking and would work very well in many situations. However, because the design is integrated into clothing, the process of reconfiguring and adding sensors with minimal hardware reconfiguration is impossible. Furthermore, their research never mentions the design of a system with flexible firmware for accepting new sensors. Another problem with the design from the standpoint of developing a truly flexible system is the exclusion of an onboard data logging feature to allow for post-experiment data processing in the event that using a computer is impractical. Of all the systems currently available for physical activity tracking, this design shows the most promise for a general purpose system. However, expandability and data logging issues still cause it to fall short of being a truly flexible system.

In addition to research groups, many companies (e.g., Nike, Polar, smart phone application developers, etc.) have developed commercial solutions for tracking motion and/or recording heart rate. These systems work well for athletes during training exercises and could be applied to certain research applications for a quick solution.

However, each of these designs has finished the development stages. None of these designs include the ability to measure environmental conditions or are capable of adapting to meet the changing needs of researchers. Thus, although they serve their various purposes well, the commercially available devices are not a substitute for the current research.

CHAPTER 3: SENSOR FRAMEWORK

The architecture of a sensor network can be designed in a number of ways. The current system is comprised of several parts. Sensor nodes placed on an individual and possibly in the surrounding environment collect data and transmit to a base node (see Figure 3.1). Notice for the example setup in Figure 3.1 that three nodes are attached to the test subject on the chest, arm, and leg. As he moves from a standing position (Figure 3.1(a)) to a sitting position (Figure 3.1(b)), notice the changes that take place in node orientation with respect to the ground. These changes and the associated movement are picked up by the sensor and transmitted to the base node. The base is then responsible for storing or transmitting the data to a computer as needed for the given application. Computer programs are then used either for post-experimental or real-time processing.



(a) Standing

(b) Sitting

Figure 3.1: Node Placement on Test Subject in Sitting and Standing Positions with Nodes on the Chest, Arm, and Upper Leg

Given proper placement of sensors, analysis of the movement data is a fairly straightforward process. Placing and picking the number of sensors is not a difficult task but requires some thought as to what type of motion the researcher is trying to track. The key is to figure out which parts of the body are expected to move during the activity. This should result in a specific number of sensors and their desired locations. For the setup shown in Figure 3.1, the leg sensor was placed just above the knee allows the researcher to tell the difference between sitting and standing. After placement has been determined, the sensors must be placed in a known orientation for a given body position in order to give the researcher a starting frame of reference. From this point, any motion at the given location will be picked up by the sensor and recorded by the system. The researcher must then use the known reference point and the data from the activity to determine what movements have taken place. As an example, using Figure 3(a) as the reference, consider the process of moving from the position in Figure 3(a) to the one depicted in Figure 3(b). The change in orientation of the arm sensor could be attributed to any number of activities, but the new position of the leg sensor indicates the horizontal orientation of the thigh associated with a sitting or lying down position. The static position of the chest sensor indicates that the subject's torso is still vertical. Therefore, the subject must be in an upright seated position. This same process can be applied to active movements (e.g., walking, running, etc.) by monitoring both positions and spikes in acceleration. If more information is needed for the particular application, this data can be further compared with environmental (e.g., ambient temperature, CO₂ concentrations, etc.) and physiological information (e.g., pulse and SpO₂) for a more complete analysis of the test results. This information allows the researcher to monitor such conditions as how

environmental factors affect physiological response, how different activities affect physiological response, and determine how much strain is associated with an activity.

The key consideration for designing all aspects of the sensor framework was flexibility. The goal was to create a design that could be easily applied to a wide variety of activities in various research applications. The current system can be easily reconfigured for deployment in different applications with minimal adjustments. New sensor nodes and types can be easily integrated into the network without the need to redesign the software or hardware. The overarching goal has been to design a sensor network capable of adapting to different situations and the changing needs of researchers. The entire framework can be divided into four categories: (1) network topology, (2) base and environmental sensor nodes, (3) personal sensor nodes, and (4) data processing.

3.1 Network Topology

Many options for sensor network topologies exist (e.g., star, mesh, ring, etc.) and could be applied to the current research (see Figure 3.2 for star and mesh examples). However, the desire to have a flexible network capable of adapting to many research projects and situations limits architecture options. The basic composition of the desired wireless sensor network includes multiple sensor nodes collecting and sending data to a base node for storage and/or processing. However, the possible desire for additional node types or changes to the communication scheme had to be considered. The topology chosen for the current research is a mesh network.

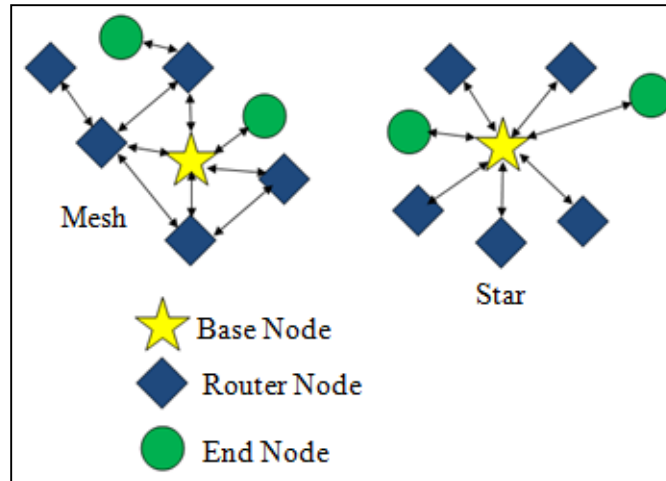


Figure 3.2: Mesh and Star Network Topologies

Given the small area generally covered by a WPSN, one could argue that a mesh network architecture is an overly convoluted solution to a simple problem. For example, a simple star topology where sensor nodes have a point-to-point connection with the base node seems to provide an adequate solution with minimal complexity. The positioning of any given sensor node on an individual's body with respect to the base node should be sufficiently small to allow direct connection to the base without rerouting data through other nodes. This is a sound argument that holds true for many research applications. However, the goal of this design is to achieve maximum system flexibility. Consider a situation in which the desire of a researcher is to monitor multiple test subjects over a large area (e.g., an entire soccer team practicing on a field). Suppose further that the researcher likes to minimize superfluous work and sources of error. Therefore, the decision is made that a central data collection point is desired to record and organize incoming data from all test subjects. Given a star topology, test subjects must limit their activities to within range of the base node. Conversely, a mesh network allows data to be routed through other sensor nodes in order to reach the base node, thus allowing

movement outside the range of the base as long as one node within range can be found. Additionally, a mesh topology also provides a more robust network. Data is not lost because a single path becomes unavailable. Multiple paths to the base allow the network to reroute data in order to avoid such failures. In a situation involving shorter distances between sensor nodes and the base, communication within a mesh may operate very similar to a star, but the mesh architecture greatly improves network stability and the flexibility of the system to adapt for a wider range of applications.

In addition to the increased sensing range and network stability, mesh networking provides another important feature. Because any given node can be aware of and communicate to any other node in the network, the system can be expanded to include new node types as the need arises. For instance, although the base node will still be responsible for data collection and/or processing, smart nodes could be included for monitoring specific conditions (e.g., heart rate, toxic gasses, etc.) and reporting dangerous situations to the wearer. Thus, the expandability of the system is improved, resulting in a sensor framework that can better adapt to the changing needs of researchers.

3.2 Base and Environmental Sensor Nodes

The base node of the framework acts as the gateway to storage and processing for all collected data. Although the Micro Fusion hardware is theoretically capable of performing these functions, it does not have the processing speed of the Fusion. If the given application requires fewer sensors and less throughput, a Micro Fusion may be used as a base. However, the capabilities of the Fusion board make it a more ideal solution for most applications. The hardware for the base node can be either a single

sensor node (Fusion or Micro Fusion) or include both the node and a computer. With the former of the two options, the base must record data from all active sensor nodes (environmental and personal) onto an SD card for future processing. Given the latter setup, the collected data is streamed directly to the computer and interpreted in real-time by the data processing software. The current design uses a personal computer for data processing. However, the Fusion could easily be reconfigured to stream data to a Bluetooth enabled device (e.g., phone, pda, etc.) running a ported version of the computer software.

In addition to its use as the base node, the Fusion is also used for the purpose it was originally intended. The framework's environmental sensing capabilities are handled exclusively by the Fusion. Due to its size, this device is not as suitable for use as wearable sensor nodes placed at multiple locations on an individual. A single Fusion attached at the waist for use as a base node/environmental sensor node works well, but the design is too bulky to wear on a limb. However, the large number of available IO, varied and numerous communication ports, high processing speed, and multiple power supply options make the Fusion an ideal vehicle for environmental sensing.

3.3 Personal Sensor Nodes

The personal sensor nodes are responsible for the motion tracking and biomedical sensing capabilities of the framework. These devices are attached to the individual and worn throughout the experiment. Although, creating miniaturized nodes for the sake of test subject comfort was not a key issue, it was considered during the design process. As previously mentioned, the Fusion is a powerful sensing platform but seemed to bulky to work as personal sensor nodes. As a low power, reduced feature set version of the Fusion,

the Micro Fusion is a much better solution. Personal sensor nodes only need to include a few sensors (e.g., accelerometers, gyros, and pulse oximeter), a microcontroller, and a radio. The Micro Fusion coupled with a sensor daughterboard easily meets these requirements and has the ability to support more sensors as needed. Sensor daughterboards can be designed and installed as needed on the Micro Fusion in order to reconfigure the system for different applications. Thus, the Micro Fusion design allows the personal sensor nodes to be a comfortable size while still maintaining the flexibility of the framework.

3.4 Data Processing

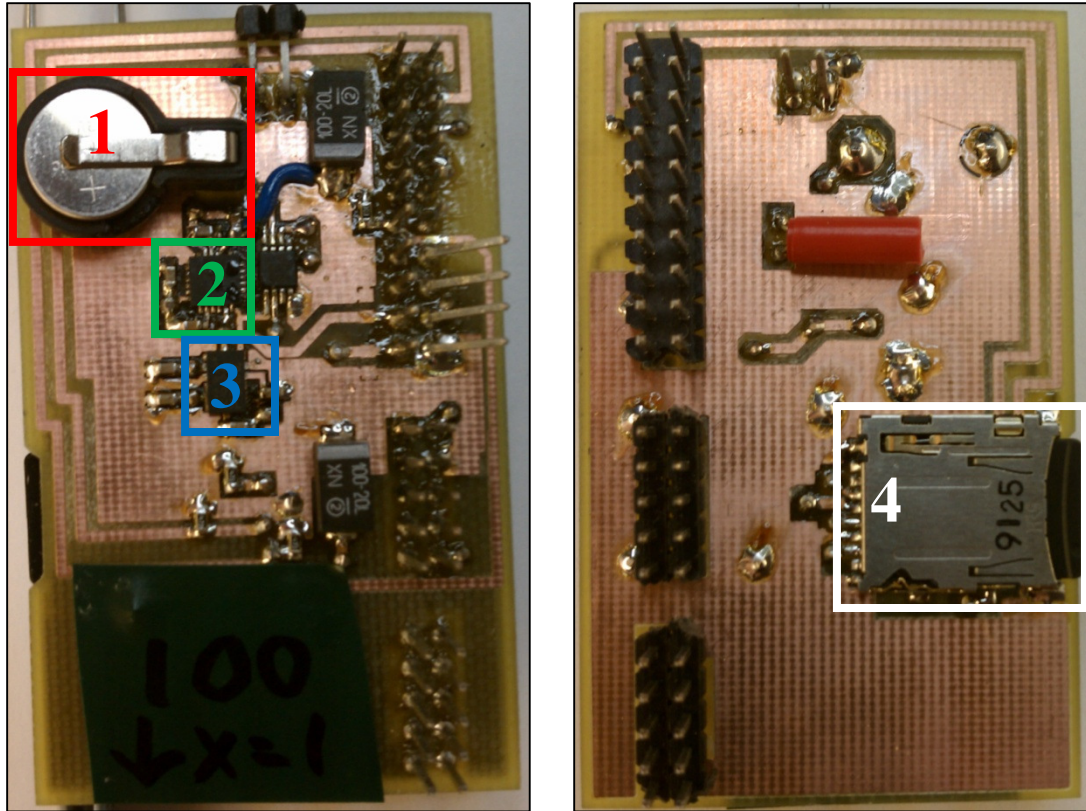
Although simple data processing can be handled by the embedded systems, the computationally intensive processing required for this research has to be accomplished on a personal computer. After being collected by the base node, the current system transmits data via a wired interface (wireless transmission is possible but not implemented) to a computer program. The program processes the received data and displays it in a graphical format in real-time. The system is further capable of storing the collected data and exporting it to a format recognizable by standard spreadsheet programs for further manipulation.

CHAPTER 4: HARDWARE DESIGN

In order to prove the viability of the Fusion and Micro Fusion motherboards for physical activity monitoring research, a system for just such a purpose had to be designed. To this end, a physical activity daughterboard was designed, a biomedical sensor system was integrated into a Micro Fusion board design, and several environmental daughterboards were created. The following sections detail the design of the system hardware.

4.1 The Micro PAD

The Micro Fusion Physical Activity Daughterboard (Micro PAD) was created, as its name suggests, for monitoring a person's movements. The board was designed to be plugged into the Micro Fusion motherboard and used with other Micro PAD's as part of a WPSN for tracking physical activity. The final design is shown in Figure 4.1 (dimensions are 3.93 x 6.33cm). The board features a real-time clock for time-stamping data, a micro-SD card for additional data storage options, and one each of a triaxial accelerometer and triaxial gyroscope for measuring movement. The design of this device is fairly simple. All devices except the micro-SD card communicate with the microcontroller via the Micro Fusion I²C port, and the micro-SD card uses SPI communication. Beyond these devices, the board includes the circuitry recommended by the device datasheets, a coin cell battery for the real-time clock for keeping time when the device is not powered, and some decoupling capacitors for filtering noise out of the supply voltage.



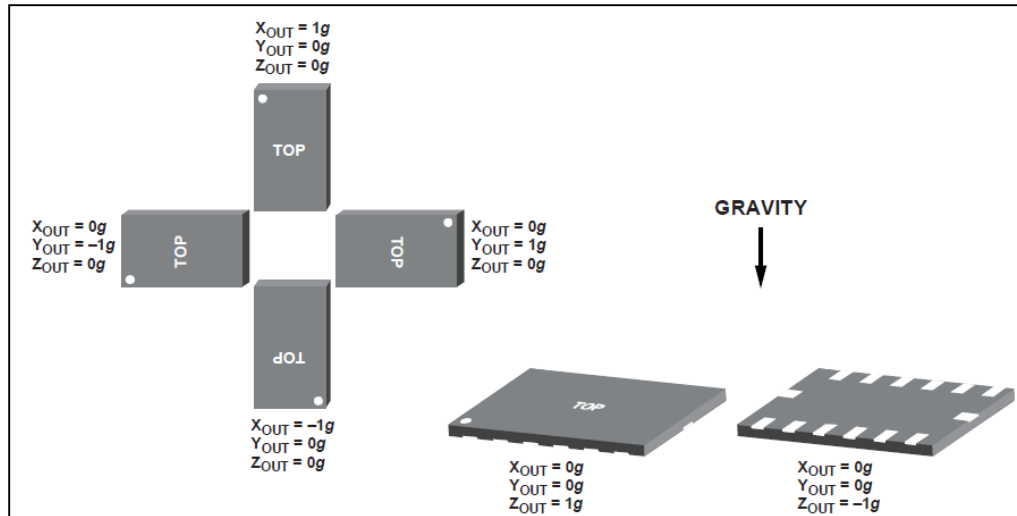
(a) Top

(b) Bottom

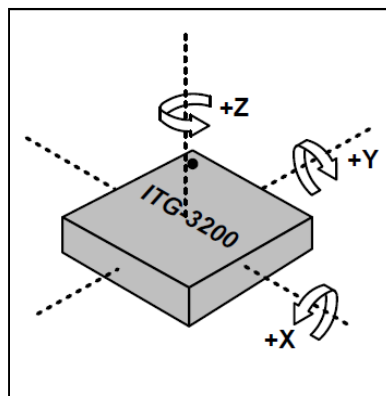
Figure 4.1: Micro PAD (3.93 x 6.33 cm)

(1) Battery; (2) Gyro; (3) Accelerometer; (4) SD Card Holder

The accelerometer and gyroscope each have three axes across which they measure acceleration. Figure 4.2(a) and Figure 4.2(b) show the orientations of the axes for the accelerometer and gyroscope, respectively. Additionally, Figure 4.2(a) shows the expected output for a given set of sensor orientations while the sensor is stationary. It should be noted that the positive direction for a given axis points opposite that of the gravity vector when the output of the sensor for said axis is 1g.



(a) Accelerometer [22] Showing Expected Axes Outputs for Static Sensor Orientations



(b) Gyroscope [23] Showing Axis Orientations

Figure 4.2: Micro PAD Axis Orientations

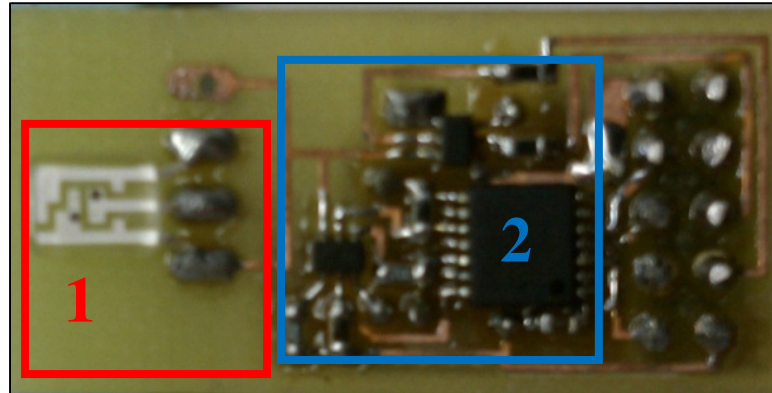
4.2 Biomedical System Design

The biomedical system could have easily been made into a daughterboard for the first revision of the hardware. However, due to the noisy nature of biomedical sensors, it was deemed desirable to eliminate error caused by noise from cable connections and long communication lines during the design process. Additionally, the biomedical system was going to include multiple sensors, but time constraints and tests performed with other sensors eventually led to the exclusion of all but the pulse oximeter.

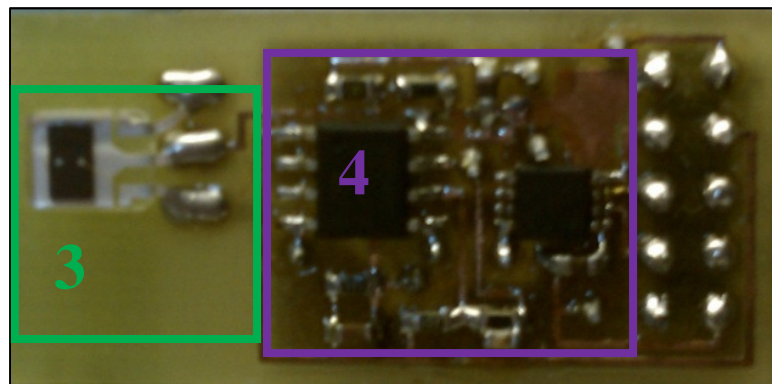
The design of the pulse oximeter sensor was based on a Texas Instruments (TI) design published in [8]. The design adheres to the basic principals as described above (see Section 1.3). The chosen light transmission devices are light emitting diodes (LED's) paired with a photodiode with a peak sensitivity encompassing the red and IR portion of the spectrum. Multiple prototypes were developed during the course of this research to adapt for changing ideas and specifications. From the first to the final prototype, the design of the LED and photodiode control circuitry did not change much if at all. The main adjustments, from a hardware perspective, were made in the microcontrollers, peripheral devices, and interface designs. The following sections detail the final designs and the important design choices.

4.2.1 Prototype 1: Pulse Oximeter

The first prototype was made for the purpose of testing the basic idea behind the design and to prove the hardware was capable of providing a useable signal. As the name of the prototype indicates, this design was simply a pulse oximeter sensor. This made the prototypes very small (dimensions are 1.63 x 3.4 cm), but they relied on the Fusion microcontroller to handle all of the signal controls and data processing. Using a tested system with more processing power than the sensor could possibly need and a pre-developed code base with extensive functionality allowed the first design to be prototyped and tested within a very short amount of time. The design can be split into two major circuits: the transmit (TX) and receive (RX) circuits (Figure 4.3(a) and Figure 4.3(b), respectively).



(a) TX Board



(b) RX Board

Figure 4.3: Pulse Oximeter Prototype (1.63 x 3.4 cm)

**(1) Dual Emitter LED; (2) TX Control Circuit; (3) Photodiode;
(4) RX Control Circuit**

The TX circuit (see Figure 4.4) is responsible for controlling the red and IR LED's. A single dual-emitter package containing both a 660nm and 880nm LED wired back-to-back was chosen in order to simplify the design process. As shown in the schematic, the design is a basic H-bridge circuit. The two PNP transistors (PNP1 and PNP2) that comprise the upper half of the "H" are controlled via general purpose input/output pins (GPIO) on the microcontroller. Operation of this part of the circuit is fairly simple as GPIO signals are either fully on or off. The interesting part of this circuit

is the lower half of the “H,” which is comprised of the NPN transistors. These are controlled via digital to analog converters (DAC’s). By adjusting the voltage at the gate of the NPN transistor, the DAC controls how much current passes from the drain to the source. Consequently, varying the output of the DAC controls the intensity of the light emitted from the LED’s.

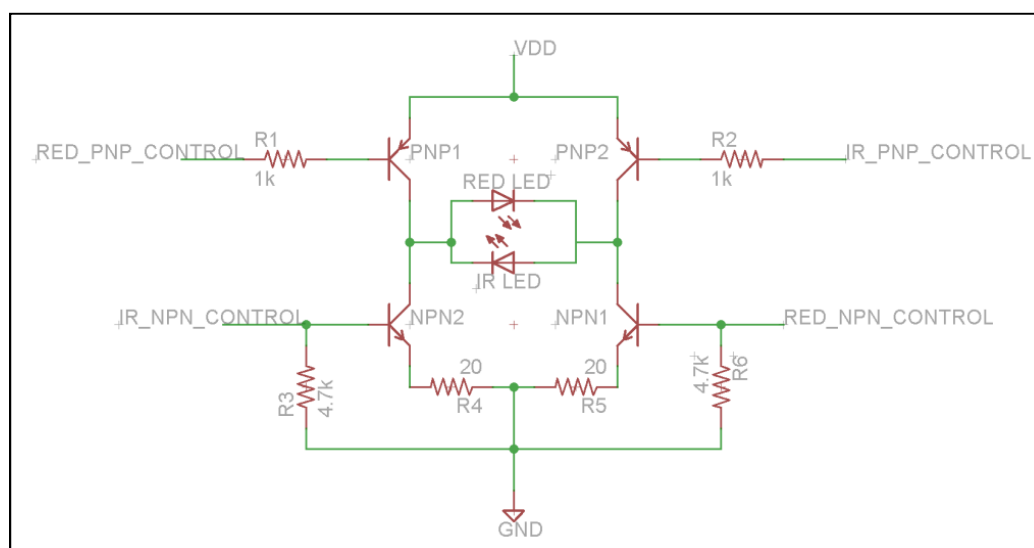


Figure 4.4: Pulse Oximeter Transmit (TX) Schematic

The RX circuit (see Figure 4.5) is slightly more complicated than the TX circuit. This portion of the design is responsible for transforming the current generated by the photodiode into a heartbeat signal that can be analyzed by the microcontroller. First, the signal from the photodiode is offset to account for the AC characteristics of a heartbeat. Then, this is fed into the first amplifier configured as a transimpedance amplifier. The transimpedance amplifier converts the current generated by the photodiode into a proportional voltage at its output. At this point, the photodiode signal can be thought of as two components: noise on top of a carrier heartbeat signal with a small DC offset. Next, the output of the transimpedance amplifier is read by the microcontroller's analog-

to-digital converter (ADC) and digitally filtered to extract the DC offset of the signal (see the Firmware Design section of this document for a more detailed discussion of this filter). The calculated offset is then fed back into the positive input of an inverting amplifier via a digital-to-analog converter (DAC). The other input of the inverting amplifier is connected directly to the output of the transimpedance amplifier. Thus, the AC portion of the signal (the actual heartbeat) is amplified, and the DC offset is effectively filtered out. The resulting signal is sent through a simple low-pass filter to attenuate some of the high frequency noise (caused by various environmental light sources, noise in the circuit, etc.) and read by the microcontroller's ADC for further filtering and analysis.

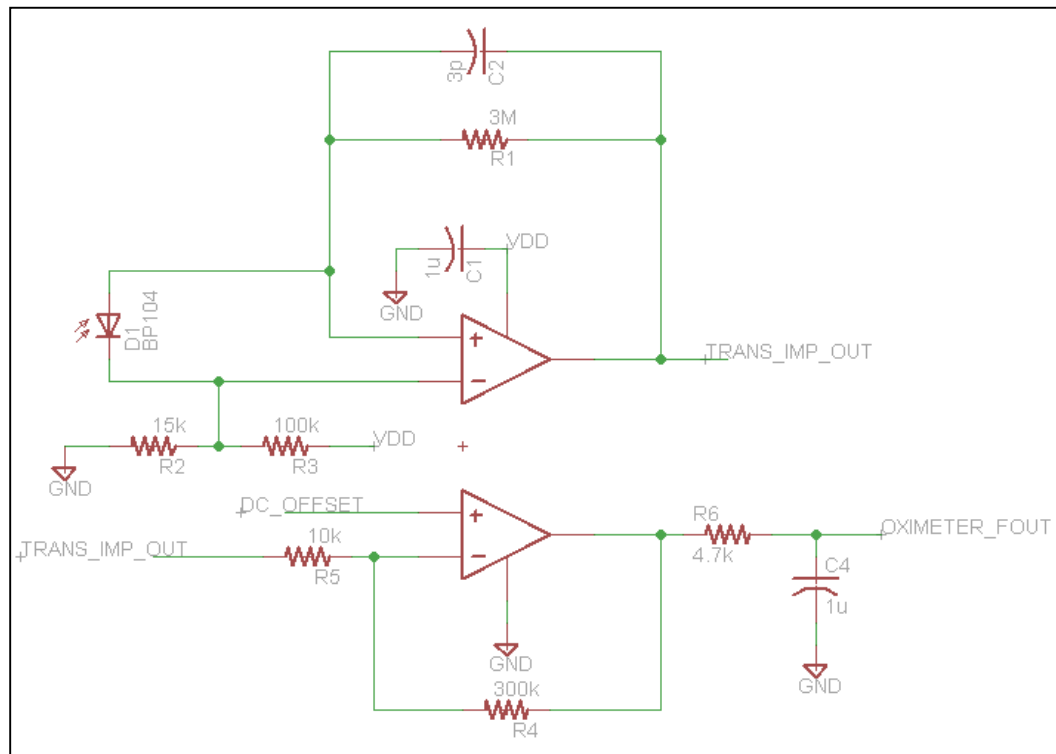
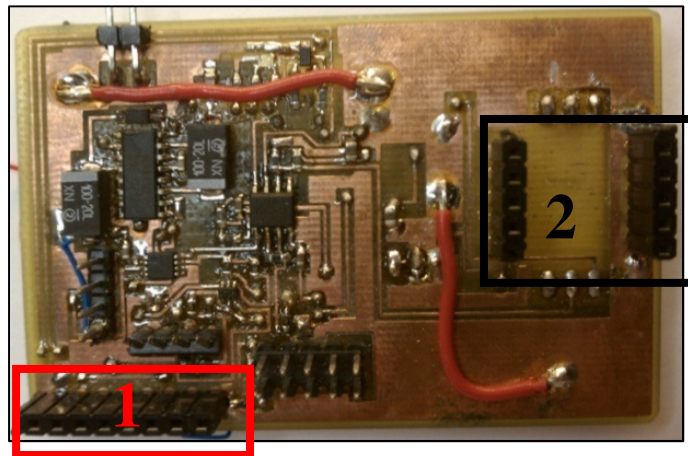


Figure 4.5: Pulse Oximeter Receive (RX) Schematic

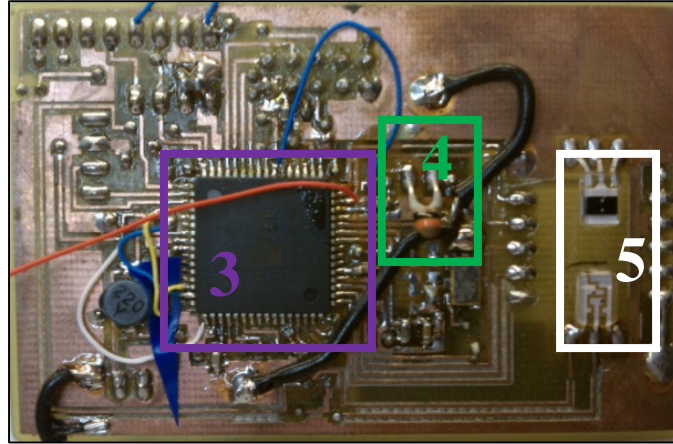
4.2.2 Prototype 2: PIP 4000

The Personal Information Processor (PIP) 4000 was the first prototype to include all necessary hardware for pulse oximetry on a signal 7.14 x 4.64 cm board (see Figure 4.6). The microcontroller chosen for the design was Atmel's ATXMEGA256A3. This 8-bit microcontroller was primarily chosen to make integration of the final design into the Fusion network simpler by making use of the existing codebase provided by the Micro Fusion project. The secondary considerations used in this determination were based on the speed of the microcontroller and peripheral devices. The ATXMEGA256A3 comes equipped with two of the three necessary DAC's, both required ADC's, and a number of communication protocol options. Furthermore, the device is more than capable of operating fast enough to support signal sampling and analysis at speeds up to 2 kHz.



(a) Top

(1) Accelerometer Header; Gyroscope Headers



(b) Bottom

(3) Microcontroller; (4) Thermistor; (5) Oximeter Photodiode and LED

Figure 4.6: The PIP 4000 (7.14 x 4.64 cm)

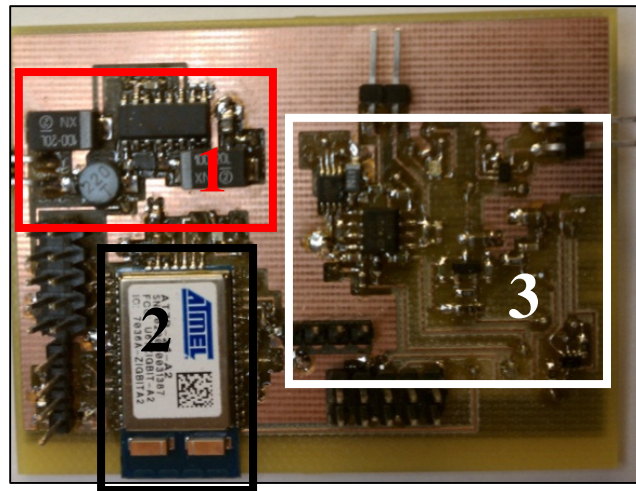
As shown in Figure 4.6 (b), even the LED's and photodiode were attached to this board. The idea for this design was to use reflective pulse oximetry on the wrist rather than transmission oximetry through the finger. Integrating the LED's into the PIP 4000 design reduced the connection length between the control circuitry and the RX/TX circuits. This reduced the amount of noise in the signal and eliminated the need for an external LED probe. However, due to increased interference caused by having little separation between the LED's and photodiode, this design proved impractical. In order to isolate the transmitted light from the photodiode, the device had to be pressed firmly into the test subject's skin. This resulted in loss of circulation and severe discomfort during extended use. Furthermore, this design did not include a wireless transmitter for integration into the Fusion network. Thus, the design was shelved in favor of a design featuring greater LED/photodiode placement flexibility and an integrated wireless transmitter.

The pulse oximeter sensor design was reused in the design of the PIP 4000. Thus, the only relevant difference between the two designs is the addition of the microcontroller. The system also included the required circuitry for additional sensors, including a gyroscope, an accelerometer, a thermistor, and a capacitive touch sensor. These failed to provide information that was of sufficient use for biomedical sensing to be considered for placement in future revisions.

4.2.3 Prototype 3: MiFOXI

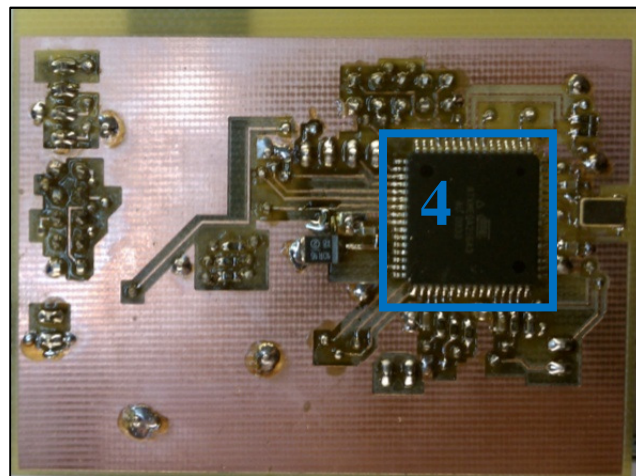
The latest version of the biomedical sensor hardware is the Micro Fusion Oximeter revision I (MiFOXI). As indicated by the name, the MiFOXI has one predecessor. The original design for the new oximeter prototype relied exclusively on the microcontroller built into a wireless radio for all data processing. During the coding process, the device was found to be incapable of performing both network operations and oximeter data processing. Therefore, the design was revised to give the oximeter a dedicated microcontroller. Figure 4.7 shows the new device (dimensions are 5.08 x 6.79cm). Although the MiFOXI is not a commercial device, some thought was still given to ease of use during the design process. All of the high profile components and various interface headers were placed on the top side of the board (see Figure 4.7(a)). This allows the device to be easily strapped to the user's arm while still granting access to the interface hardware. This was also true of the previous prototype (PIP 4000), but that device also had to accommodate the placement of the LED's and photodiode. As previously noted, the PIP 4000 was created to use reflectance pulse oximetry on the wrist. In order to try new placements and the more traditional transmission oximetry, more flexibility was desired. This was achieved by using a header interface (see Figure 4.7(a))

and Figure 4.7(c)) in place of the actual LED's and photodiode. This feature of the design allowed the LED's and photodiode to be packaged into any desired configuration and made the testing of different placements on the same control hardware possible. See Figure 4.7 (c) for an example of a LED/photodiode probe connected to the MiFOX1.



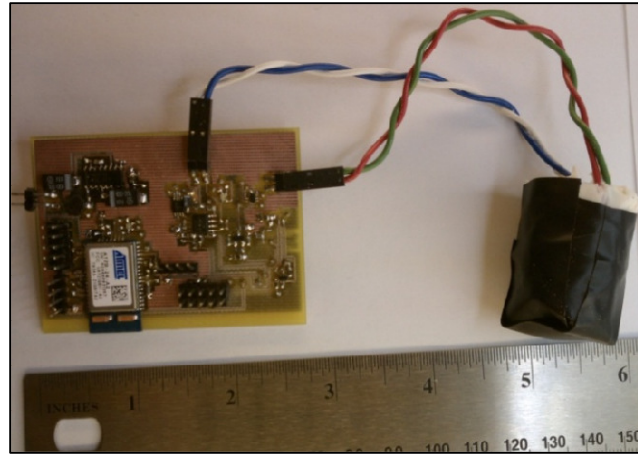
(a) Top

(1) Power Supply; (2) Zigbit Radio; (3) Pulse Oximeter Control Circuit



(b) Bottom

(4) Microcontroller

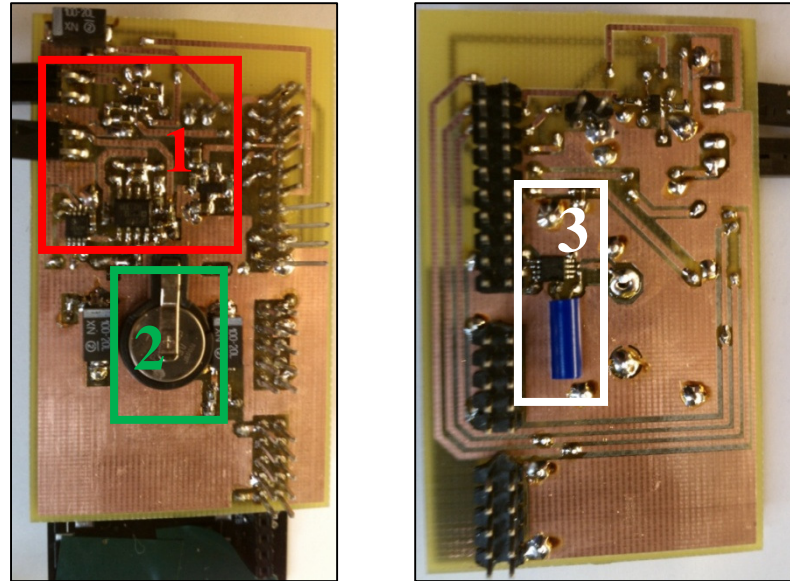


(c) Board with LED Finger Probe

Figure 4.7: The MiFOXI (5.08 x 6.79 cm)

The MiFOXI design is similar to the PIP 4000 with two significant exceptions. First, the superfluous additional sensors are no longer included in the MiFOXI. Second, the device was designed to incorporate Atmel's Zigbit radio (outlined in blue). The Zigbit allows the oximeter to communicate with any Fusion network via the Zigbee wireless protocol.

At this stage of the design process, it was deemed feasible to rework the prototype into a daughterboard for the Micro Fusion platform. As previously mentioned, the microcontroller for the pulse oximeter designs was chosen in part because it was the same device used in the Micro Fusion. Thus, redesigning the MiFOXI into a daughterboard required very little effort. The final design for the Micro Fusion Oximeter rev I Daughterboard (MiFOXI Daughter) can be seen in Figure 4.8. The dimensions for the new design are smaller (6.93 x 4.27cm), making it a perfect fit for the Micro Fusion platform.



(a) Top

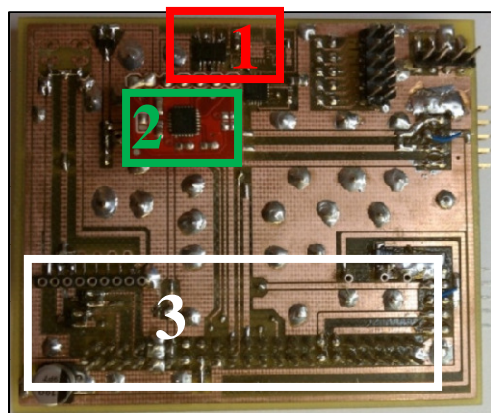
(b) Bottom

Figure 4.8: MiFOXI Daughter (6.93 x 4.27 cm)

(1) Oximeter Control Circuit; (2) Battery; (3) Real-Time Clock

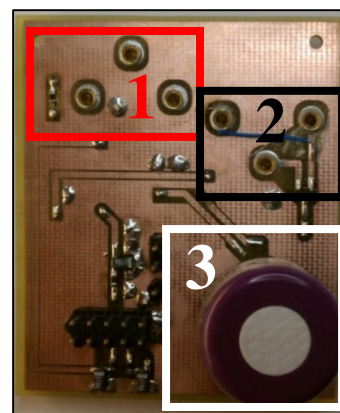
4.3 Environmental Sensor Daughterboards

Several environmental sensor daughterboards were developed as a means of testing the functionality of the Fusion motherboard (see examples in Figure 4.9). Due to the resources provided by Fusion, the designs for these boards are very simple. Each board requires only the desired sensors, their specific circuitry, and a header for interfacing with Fusion. As described in Section 2.1, the motherboard supplies all generic necessities. If a particular sensor needs a more specialized supply voltage or outputs a signal higher than 3.3V, more specialized circuitry may be required.

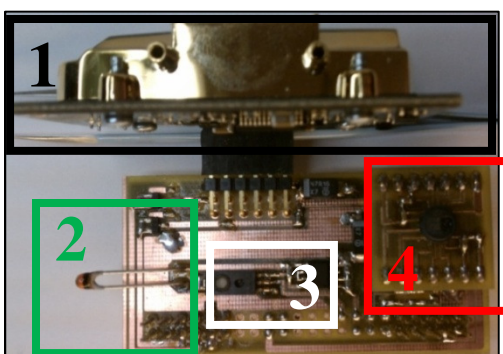


(a) Fusion Unleashed (6.72 x 7.95 cm)

(1) Accelerometer; (2) Gyro; (3) Headers



(b) CONFusion (5.05 x 5.98 cm)

(1) CO₂; (2) O₂; (3) NH₃

(c) Fusion the HuT (3.19 x 6.24 cm)

(1) CO₂; (2) Temperature; (3) Humidity; (4) Atmospheric Pressure**Figure 4.9: Environmental Sensor Daughterboards**

The example boards shown in Figure 4.9 are some of the first prototype daughterboards built for the Fusion. Figure 4.9(a) shows the Fusion Unleashed breakout board (dimensions are 6.72 x 7.95cm). This design incorporates the accelerometer and gyroscope from the Micro PAD design, but its primary purpose was to create a simpler interface for boards using the I²C interface. The angled headers on the right side of the board include the 3.3V, $\pm 5V$, ground, and I²C communication signals. The idea for this is to have a long ribbon cable with multiple terminations that allow various I²C based daughterboards to be swapped in and out of the system as a particular application

requires. Figure 4.9(b) is an example of one I²C based daughterboard. The Carbon monoxide, Oxygen, and Ammonia (NH₃) Fusion daughterboard (CONFusion) is capable of sensing the three gasses in its name and reporting the concentrations back to the Fusion motherboard for processing. Other daughterboards similar to this could easily be designed and used to sense any number of environmental factors. The size of these boards is determined by the type and number of sensors. The size of the CONFusion is approximately 5.05 x 5.98 cm. As another option, the daughterboard depicted in Figure 4.9(c) was designed to be a more compact sensing solution (dimensions are 3.19 x 6.24 cm). The device requires no external cabling and attaches via male headers directly to Fusion (eliminating the need for an interface board). The Fusion Humidity and Temperature daughterboard (Fusion the HuT) is actually capable of sensing humidity, temperature, CO₂, and atmospheric pressure. By connecting directly to the motherboard without an interface board (e.g., Fusion Unleashed), a smaller size can be maintained. Similar daughterboards could be created for applications in which size is a primary concern.

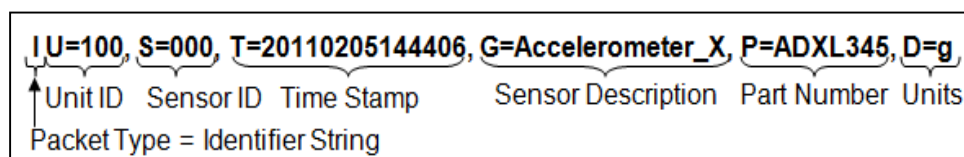
CHAPTER 5: SOFTWARE DESIGN

The software design for the current research, although aided by the Hartman Systems Integration Lab codebase, was still a significant challenge. Each new sensor added to one of the two motherboards required its own specific code module within the firmware, and computer programs for real-time and post-experiment data processing had to be developed. The following sections outline the design of the firmware and software created for the current research.

5.1 Micro PAD Firmware

The Micro PAD firmware is fairly simple because it takes full advantage of the resources provided by the code developed for the motherboard. The Micro Fusion firmware uses a timer-driven sensor scheduling scheme. Upon startup the system initializes all communication protocols and the timer system. Next, the code traverses its list of enabled sensors, initializing each one with the desired settings and stores and/or transmits each sensor's identifier string (see example in Figure 5.1(a)). In the case of the Micro PAD sensors, the current time is read from the real-time clock in order to set the system time, and the accelerometer and gyroscope are set to continuously record measurements at the highest resolution available for each device. As the final stage of each sensor's initialization routine, a measurement function is registered with the scheduler to be called at a regular interval (1-2Hz for the gyroscope and accelerometer). When the function is called, a flag is set high, and the measurement is read via I²C communication at the microcontroller's earliest convenience. At this point, the

measurement is time stamped and formatted into a measurement string as shown in Figure 5.1(b). Finally, the data is stored and/or transmitted to a base node for further processing.



(a) Identifier String



(b) Measurement String

Figure 5.1: Fusion Network Data Format Strings

The data format strings shown in Figure 5.1 were carefully developed for sensor networks. The decision to create a separate identifier string was made in order to reduce the amount of information that had to be transmitted with each measurement. The identifier gives the researcher or data processing program important information such as a description of the sensor, its part number, the units it measures, the time it joined the network, and a unique set of two numbers that serve as its identity on the network (see the Unit ID and Sensor ID in Figure 5.1(a)). The Unit ID is a number that is unique to each node on a network, and the Sensor ID is unique to each sensor on a node. Every sensor generates an identifier with these two numbers, and they are included on every measurement string (see Figure 5.1(b)). Thus, each measurement can be matched with its identifier, and the information in the identifier only has to be transmitted once.

5.2 Biomedical System Firmware

The pulse oximeter firmware is a sensor specific module that is added to the Micro Fusion motherboard firmware as described in Section 5.1. However, this sensor is controlled via its own timer rather than the system scheduler in order to meet the demanding time constraints. The sensor specific code plays a significant role in the performance of the device. The algorithms can be split up into five main functions:

- LED Control
- DC Tracking
- Signal Filtering
- Peak Detection
- Pulse and SpO₂ Calculation

The first two functions are the most critical to device operation and are handled entirely within a timed interrupt service routine (ISR). If either of the first two algorithms is implemented incorrectly, the output from the final amplification stage will be meaningless noise. Although the last three are necessary for processing the signal into usable data, they are not nearly as critical. Thus, they are handled by a sensor task called from the main program loop. Figure 5.2 shows a block diagram of the firmware system and its interaction with some of the hardware (shown outlined in red).

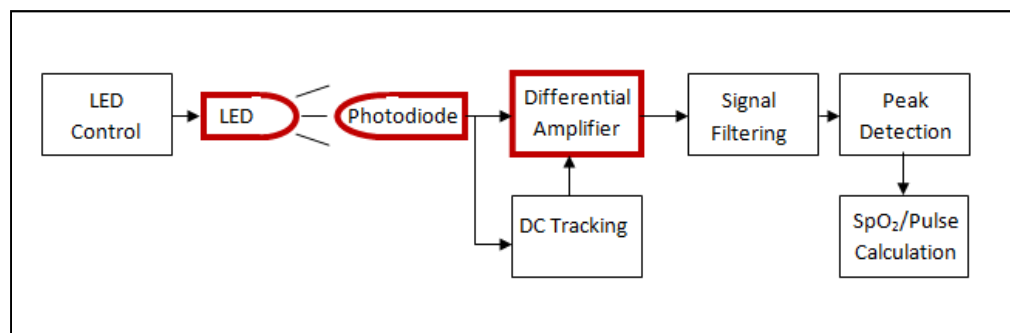


Figure 5.2: Pulse Oximeter Firmware Block Diagram Showing Hardware (Red Outline) and Software (Black Outline) Blocks

5.2.1 LED Control

Controlling the multiplexing of the LED's is a fairly straightforward process. The basic operation involves the use of a simple 4-position state machine triggered off of a timer. Research of other designs [7, 8] and experimentation showed the desired sample rate to be around 500 Hz-1 kHz for each LED. Two LED's multiplexed and sampled at 1 kHz could theoretically be clocked off of a 2 kHz timer. However, the sampling operation consists of more than just toggling an LED and reading a value from the ADC. If the ADC is sampled directly after turning on an LED, the system has a high probability of taking a measurement while the LED is turning on or still in an off state. Another important potential problem to consider is the possibility of creating a short to ground through the H-bridge circuit (see Figure 4.4). If the transistors controlling one LED are not given adequate time to turn off before the next set of transistors turns on, there is a risk of having all four transistors being on at once. This would result in damaged hardware. To avoid such problems, the current system turns on an LED (state 0) and waits for 3 timer ticks before taking a measurement and turning off the first LED (state 1). The system then waits for 1 more tick before turning on the next LED (state2) and taking its measurement after another 3 tick waiting period (state 3). The entire process spanning 8 timer ticks is repeated as long as the system is running. Because the chosen sample rate is 1 kHz and the state machine requires 8 ticks, the timer is set to trigger ticks at a rate of 8 kHz.

Another essential part of LED control is the adjustment of light intensity. As shown in Figure 4.5, the LED's share a common receive circuit. Although each LED gets its own set of filtering and processing algorithms, the hardware does not handle each

separately. Figure 5.3 shows the spectral responsivity of the photodiode. Notice that the responsivity of the device is a little more than 1.5 times higher for the 880 nm light than it is for the 660 nm light. Thus, if the intensities of the IR and red LED's are equal, the output from the photodiode will be greater when the IR LED is emitting. Consequently, the DC tracking value will be higher 50% of the time. This will cause the output of the system to become unstable and inject noise whose amplitude can match or exceed the heartbeat signal. In order to correct this problem, the intensities of the two LED's must be adjusted such that the DC levels of the corresponding signals generated by the photodiode match. Currently, this is done by hard coding the value sent to the DAC responsible for controlling the red LED to be larger (by approximately 1.5 times) than the value sent to the DAC controlling the IR LED. In the future, this could be accomplished using an algorithm that compares the DC levels of each signal and adjusts the DAC values accordingly. This solution would be far more elegant and allow for more automated control of the system possibly making it more robust.

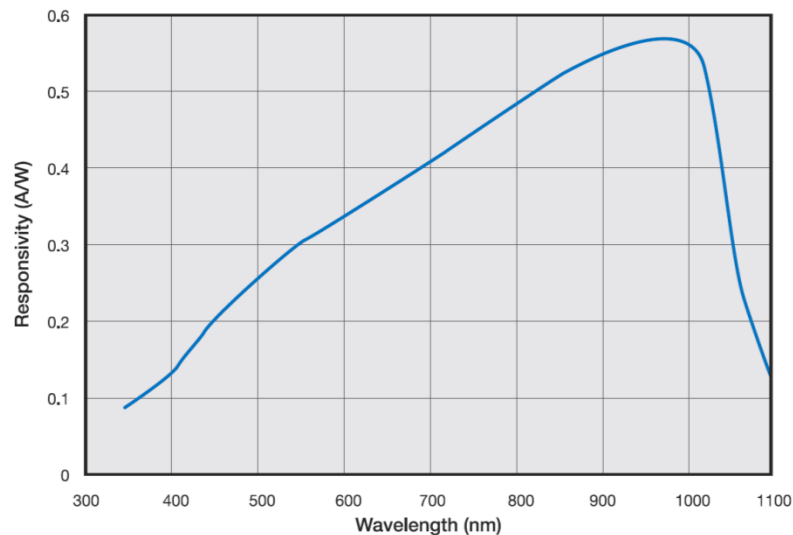
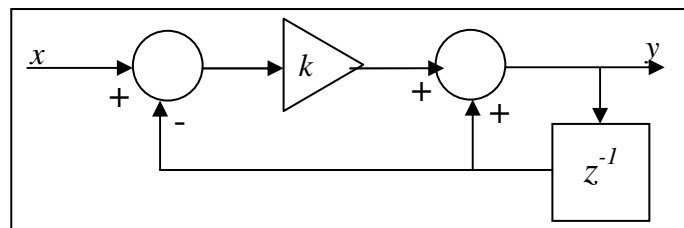


Figure 5.3: Spectral Responsivity of the Photodiode [24]

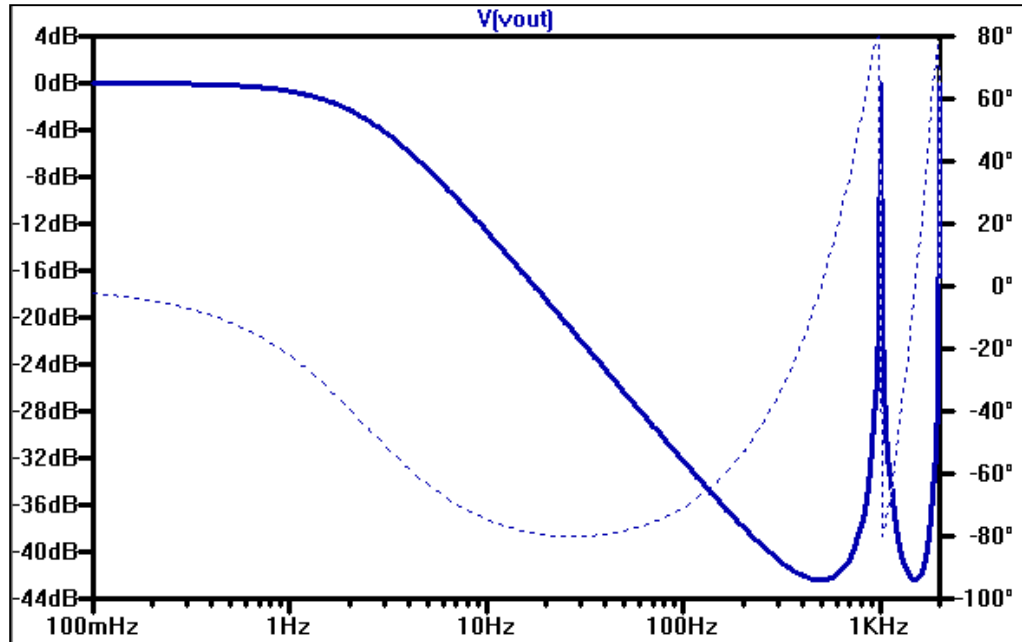
5.2.2 DC Tracking

DC tracking is essential to the operation of the second stage of amplification. The firmware uses a simple infinite impulse response (IIR) filter to accomplish this task. Equation 2 shows the transfer function of the IIR filter, and Figure 5.4(a) shows its block diagram. The basic operation of the filter is to add a fraction of the difference between the previous output and current input to the previous output. This results in a new output that changes to match the input over a period of time where the rate of change is controlled by the "fraction of the difference" used (see k in Figure 5.4). By making k sufficiently small ($k < 1$), the output can be made to ignore the AC component of the heartbeat signal. Thus, only the DC offset of the heartbeat signal is outputted to the second stage of amplification [8].

$$H(f) = \frac{1 + j2\pi \times f / 1000}{1 + j2\pi \times f / (1000 \times k)} \quad (2)$$



(a) Block Diagram [8]



(b) Magnitude (—) and Phase (···) Response

Figure 5.4: DC Tracking Filter Design and Performance Figures

It should be noted that special care had to be taken in implementing digital filters and selecting a value for k on the current hardware. The ATXMEGA256A3 is not a digital signal processor (DSP) chip and should not be treated as one. This microcontroller handles floating-point operations in software because it has no dedicated floating-point hardware. Consequently, each floating-point operation costs a significant number of clock cycles. Given that the current algorithms rely heavily on completing critical DC tracking calculations inside the ISR, reducing the number of floating-point calculations was a necessity. Another potential pitfall to be aware of when working with digital filters in this system (or any system for that matter) is the possibility of errors in calculations. For example, consider the DC tracking filter shown in Figure 5.4. This filter should be stable for the value of $k = 0.002$ suggested in [8]. However, the filter is only marginally stable on the MiFOX1 for this value given a floating-point resolution of 16 bits. This

issue made for interesting troubleshooting until the filter's variables were switched to double precision floating-point variables (32 bits). Increasing the resolution made overflow errors less likely and improved system stability. As a further precaution, k was increased in order to move the pole of the filter further inside the unit circle. The current value of k being used is 0.015. The frequency response of the filter for $k = 0.015$ is shown in Figure 5.4(b).

5.2.3 Signal Filtering

Noise is more often than not the bane of circuit design. A circuit whose simulations show perfect operation can be rendered useless by noise stemming from a myriad of sources ranging from environmental to un-intended antennas created during layout. This rule holds true for the oximeter design (see Figure 5.5). The photodiode is expected to sense a low frequency heartbeat (approximately 1-4 Hz) and generate the corresponding signal. However, the photodiode is not exclusively sensitive to the red and IR wavelengths (see Figure 5.3). Standard home/office light sources also trigger current generation and introduce high frequency noise into the generated signal. Furthermore, non-ideal circuit layout and components (DAC's, operational amplifiers, etc.) also add noise to the system. One good solution to this problem is digital low-pass filtering of the heartbeat signal.

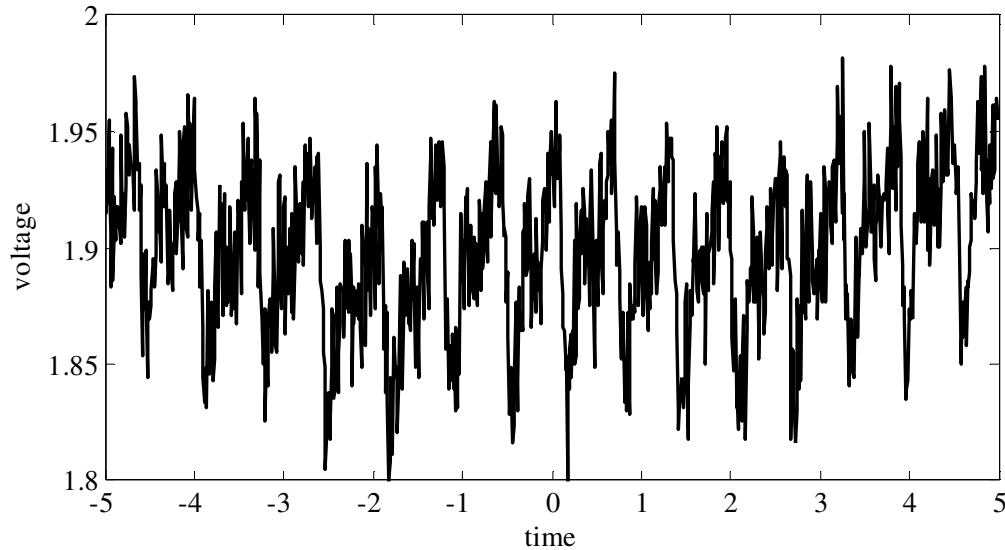


Figure 5.5: Heartbeat Signal Before Digital Filtering

Designing a digital low-pass filter for the pulse oximeter design was simple due to the large difference between the frequency of the desired signal and the frequency of the unwanted noise. Close analysis of the noise seen in Figure 5.5 revealed the major components have a frequency between 60 Hz and 120 Hz. The first design considered was a simple moving average filter. However, a moving average filter required too many floating-point operations and consumed a lot of memory. Furthermore, the benefit realized by this design would not have adequately removed the noise from the heart beat signal. Thus, a more complicated design was required. The final design was an IIR second order Butterworth filter implemented in a direct-form II second-order-section. The block diagram for this filter is shown in Figure 5.6. Equations 3 and 4 show the mathematical translation of the diagram used to implement the filter in the algorithm.

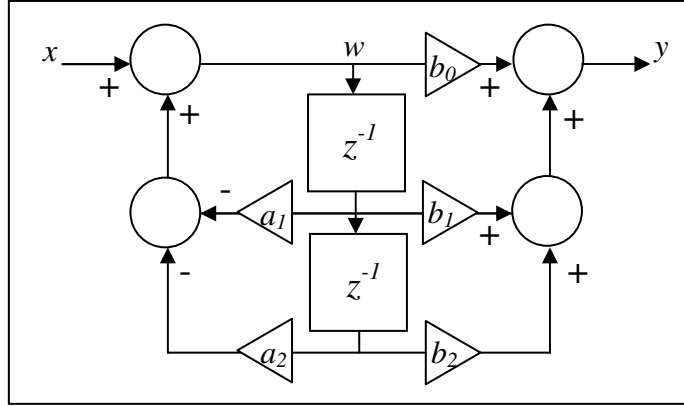


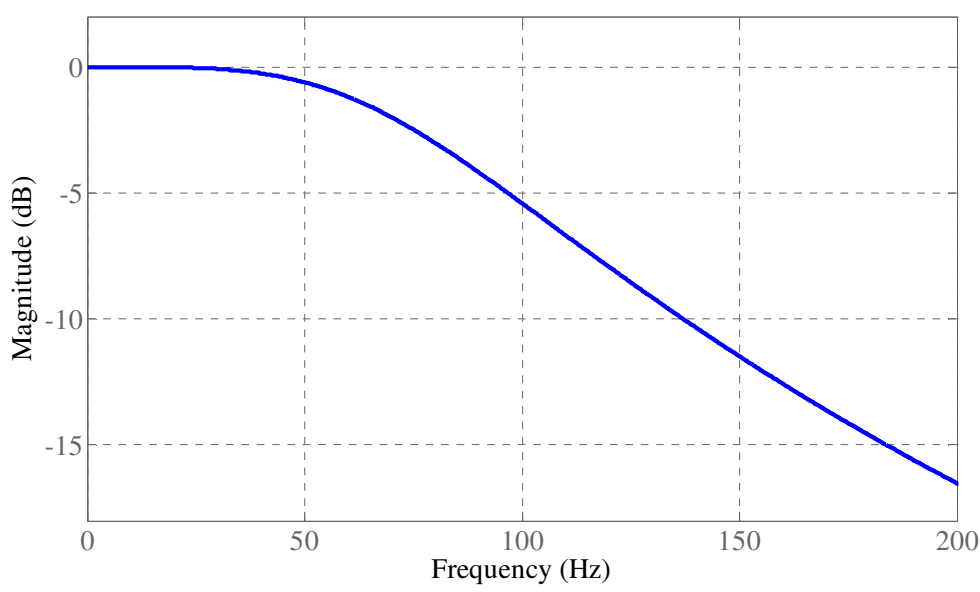
Figure 5.6: Butterworth Second Order Filter Block Diagram

$$w = x - a_1 w(z^{-1}) - a_2 w(z^{-2}) \quad (3)$$

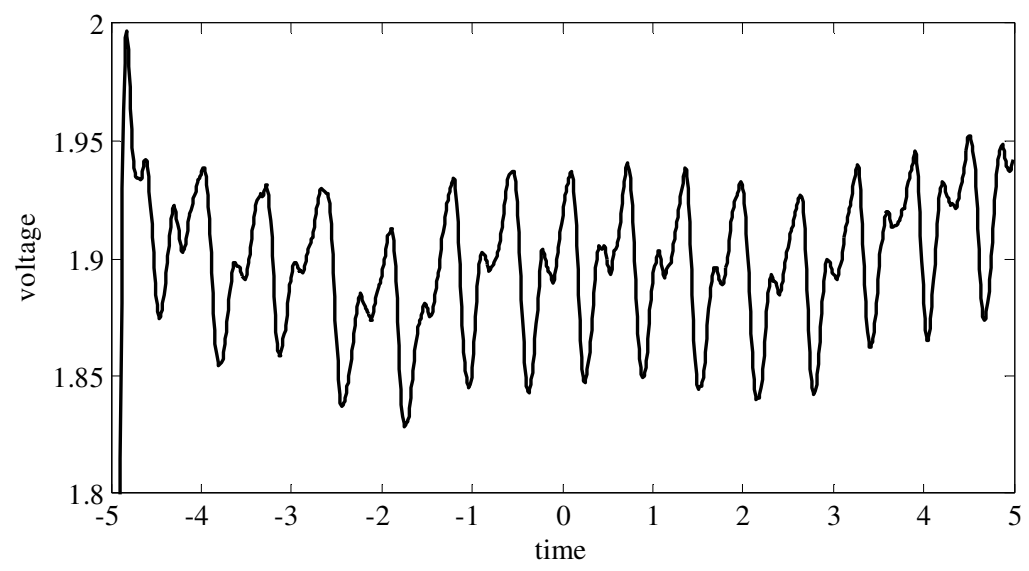
$$y = G * (b_0 w - b_1 w(z^{-1}) - b_2 w(z^{-2})) \quad (4)$$

The values of the filter shown above (where G is the gain) were chosen such that the cutoff frequency was approximately 40 Hz. Equation 5 shows the transfer function for the filter (where $a_1 = -1.647459$, $a_2 = 0.700896$, $b_0 = 1$, $b_1 = 2$, $b_2 = 1$, and $G = 0.013359$). Keeping the cutoff frequency at this value allows the filter to remove the unwanted noise without attenuating the original signal (see the magnitude response in Figure 5.7(a)). Simulations in Matlab showed this design to be far more effective at noise removal. Figure 5.7(b) shows the heartbeat signal from Figure 5.5 after being filtered.

$$H(f) = G \times \frac{(1 + j2\pi f/1000)^2 + b_1(1 + j2\pi f/1000) + b_2}{(1 + j2\pi f/1000)^2 + a_1(1 + j2\pi f/1000) + a_2} \quad (5)$$



(a) Magnitude Response of the LPF



(b) Filtered Heartbeat Signal from Figure 5.5

Figure 5.7: Digital LPF Magnitude Response and Filtered Heartbeat Signal

5.2.4 Peak Detection

The first step of data processing is the peak detection algorithm. In order to complete pulse and SpO₂ calculations, the number and magnitude of the peaks created by both LED's must be known. The method for detecting peaks is a three-stage process. The

first stage is the digital LPF discussed in the previous section. Once the signal is cleaned up by the LPF, it is passed to a DC tracking filter like the one discussed in the Digital Tracking section above (henceforth referred to as the Pulse DC tracking filter). The final stage is a two position state machine whose purpose is to track the characteristics of a pulse.

As shown in Figure 5.7(b), a pulse is characterized by a slow rise to a peak followed by a quick drop. Another distinctive feature that can be seen in the figure is the double peak on each pulse. Detecting this double peak would be a great way to distinguish the heartbeat signal from low frequency noise. However, given a weaker heartbeat signal, this feature is not always present. Luckily, as long as the system is stable, thresholds can be used to ignore the low frequency noise as it has a much lower amplitude than the desired signal. Thus, thresholds are set above and below the DC level of the heartbeat signal to detect the beats and distinguish them from any low frequency noise that might be present. The first position of the state machine checks if the current signal is above the value calculated by the Pulse DC tracking filter by a predetermined threshold (approximately 10mV). Until this is detected, a variable, min-var, is checked against the current signal and updated if a lower value is detected. Once the threshold is detected, min-var holds the minimum value sensed during the pulse and the state machine moves to the second position. The second position checks if the current signal is below the value calculated by the Pulse DC tracking filter by the same predetermined threshold. Until this is detected, another variable, max-var, is checked against the current signal and updated if a higher value is detected. Once the threshold is detected, max-var holds the highest value sensed during the pulse, a pulse counting variable is incremented, and the

state machine returns to the first state. At this point, enough data has been collected to calculate the pulse and SpO₂.

5.2.5 Pulse and SpO₂ Calculation

The pulse calculation is the simpler of the two calculations. It also requires less hardware. The pulse is calculated based entirely off of the signal generated by the photodiode detecting the light from the IR LED. Although either wavelength could be used to calculate the pulse, the photodiode is more sensitive to the IR wavelength, and IR light is attenuated less by bodily tissues. Consequently, the signal generated from detecting the IR light has a greater amplitude. Three algorithms were developed for handling pulse calculation. The first was a simple, inaccurate design developed as a proof of concept. A timer was used to count off a ten second interval. At the end of this interval, the number of pulses counted by the peak detection circuit (see previous section) and multiplied by 6. The limitations of the algorithm are readily apparent. It gets a reading quickly but can show an accurate pulse only if it is a multiple of 6. This solution served its purpose but needed a more accurate replacement. The second solution was to just count the number of beats detected in the past minute and display that result. This was an accurate method of determining the heart rate, but it takes at least a full minute to get an accurate reading. Thus, the third algorithm was created in a similar fashion to the first. The basic operation is to first count the number of samples taken in the time it takes to sense 3 heartbeats. Then, use Equation 6 to calculate the pulse. This method of calculation gets a reasonably accurate reading in the time it takes the user's heart to beat 3 times.

$$\text{Heart Rate} = \frac{\text{Samples}}{\text{Minute}} \times \frac{3 \text{ Beats}}{\# \text{ of Samples Taken in 3 Beats}} \quad (6)$$

Although not overly complex, the SpO₂ calculation is a little more involved. First, a ratio of the amplitudes and DC levels of the detected IR and red LED signals must be calculated using Equation 7. This is accomplished using the min-var, max-var, and Pulse DC tracking filter values recorded by the state machine for each LED. If the DC levels of the signals produced by each LED are properly matched, they can be removed from Equation 7 to further simplify the process. Once the ratio calculation is done, Equation 8 is used to calculate the SpO₂. This equation is derived using Beer-Lambert Law (see Equation 1). The values for the constants are found empirically. This is usually accomplished by using specialized hardware that imitates a person's finger with different SpO₂ levels. The reason for the different levels of calibration is to account for the ability to detect abnormal or dangerous blood oxygenation. However, this lies outside the scope of this project. This design was meant to be used on healthy individuals to detect fluctuations in SpO₂. Thus, calibration using a healthy test subject's finger within the normal range (90%-100%) is sufficient.

$$R = \frac{\text{Red_Amplitude/Red_DC}}{\text{IR_Amplitude/IR_DC}} \quad (7)$$

$$\text{SpO}_2 = 100 \times \frac{0.81 - 0.36R}{0.68 - 0.22R} \quad (8)$$

5.3 Environmental Sensor Firmware

As previously discussed in Section 2.1.3, the firmware for the two motherboards was designed such that the high level code could be easily ported from one system to the other. As such, the description of the sensor scheduling described in Section 5.1 can be

applied to the environmental sensing system as well. Each sensor on the various environmental daughterboards has its own module of sensor specific code inside the Fusion firmware. Depending on the type of sensor, this code can be as simple as an I²C measurement reading (as in the Micro PAD sensors). Although the communication interfaces vary, the code for most sensors is this simple. However, a few of the gas sensors require additional code to create drive signals for more complicated circuitry (e.g., the CO₂ sensor). For these sensors, additional code is written upon initialization to schedule toggling of the requisite GPIO pins.

Beyond the sensor scheduling, one node of the environmental system is also responsible for handling the data transmitted across the network. As previously mentioned, the Fusion motherboard, which serves as the environmental sensing platform, is configured as the network base node for the current research. In order to handle these responsibilities, the Fusion is equipped with a "Data Manager" module. Depending on the configuration set by the researcher for incoming data, the Data Manager routes incoming data to the desired destination: UART (computer), SD card, or both.

5.4 Computer Software

Storing data to an SD card or displaying it on a HyperTerminal program is fine for the early stages of testing a prototype, but more powerful tools are needed for actual data processing. Whether data analysis is being done in real-time or after the experiment is completed, the ability to graphically display and manipulate data is usually required. For this reason, two general purpose data graphing tools have been developed for use with the Fusion network.

5.4.1 BSU Sensor Graphing Utility

The BSU Sensor Graphing utility was designed as a simple tool for post-experiment data analysis. The program reads the measurement and identifier strings from a file stored on a Fusion or Micro Fusion SD card or from a log file captured by the BSU Sensor Monitor Lite program (see Section 5.4.2). The strings are parsed, and data is organized by the Unit and Sensor ID's (see Figure 5.1). Once this is complete, a user may select any of the sensors (by description and Unit ID) from the drop-down list as shown in Figure 5.8. A graph of the data for the selected sensor is generated and displayed with the axes limits automatically set such that all data is visible. Clicking the "Options" pull-down menu item or double-clicking the graph will open a dialog box allowing the user to select the color of the displayed data, adjust the axes limits, and enable/disable the auto scaling feature. Axes limits may also be adjusted by using the scroll wheel on a mouse with the cursor held over the graph. While all of these features are useful, it may still be desirable to create custom graphs using multiple sensors or small pieces of a dataset. In order to facilitate this process, BSU Sensor Graph has two procedures. First, if the data has already been processed by the utility, the "Export" button at the bottom left of the window can be used to create a ".csv" version of the data that can be opened in any spreadsheet program (e.g., Microsoft Excel). The second option is to click on the "Bulk Process" menu option in the "File" menu. This generates an "Open File" dialog that allows the user to select any number of data files for processing. Once selected, BSU Sensor Graph will generate ".csv" versions of each selected file.

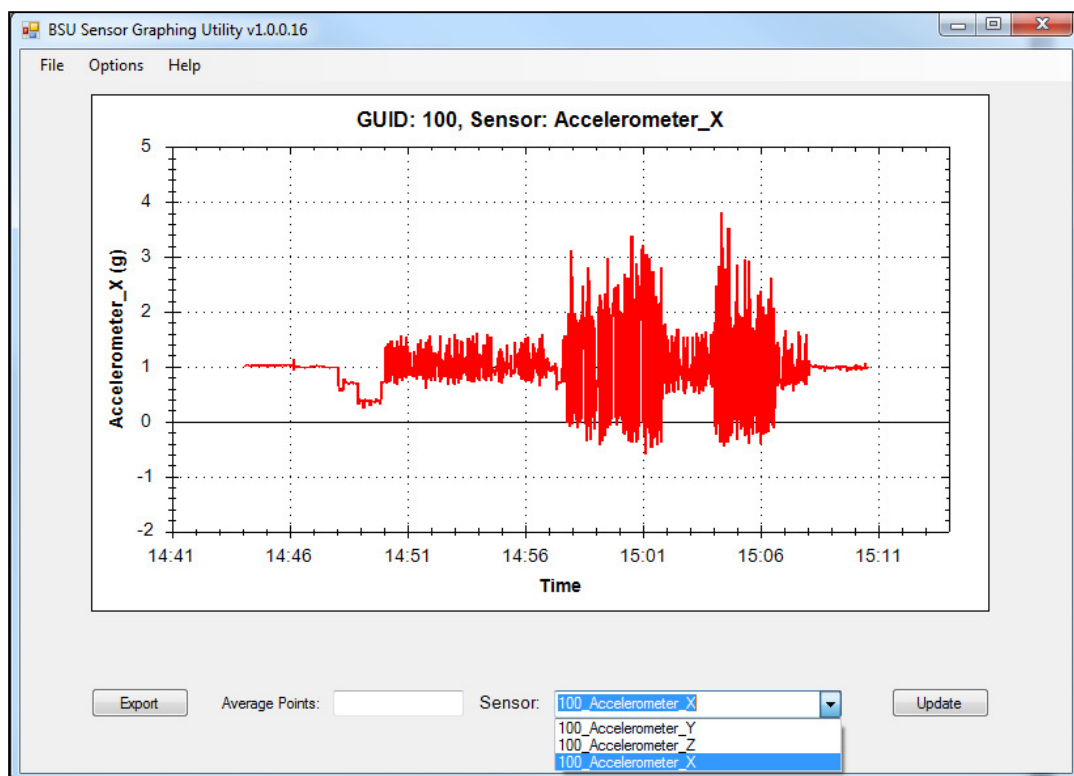


Figure 5.8: BSU Sensor Graphing Utility Screenshot

5.4.2 BSU Sensor Monitor Lite Program

The real-time data processing counterpart of the BSU Sensor Graphing Utility is the BSU Sensor Monitor Lite program. The graphical interface for both programs is extremely similar (see Figure 5.9), and the BSU Sensor Monitor Lite program incorporates all of the functionality of its counterpart. In addition to the post-experiment data processing features, the BSU Sensor Monitor Lite program also allows users to set up one of the computer's Comm ports to record data from a Fusion or Micro Fusion motherboard. Data transmitted from the device to the computer is logged into a text file automatically and can be graphed in real-time. Finally, at the end of the experiment, the program creates a ".csv" version of the data before it closes to allow for further analysis and processing in a spreadsheet program.

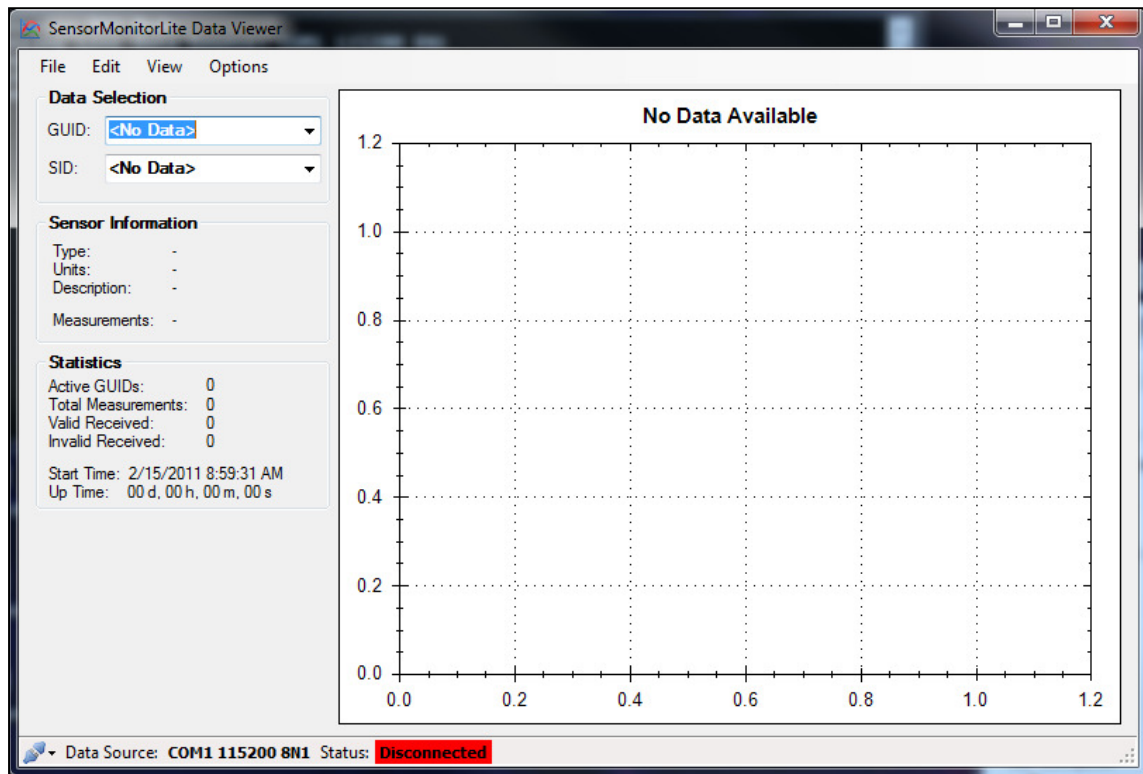


Figure 5.9: BSU Sensor Monitor Lite Program Screenshot

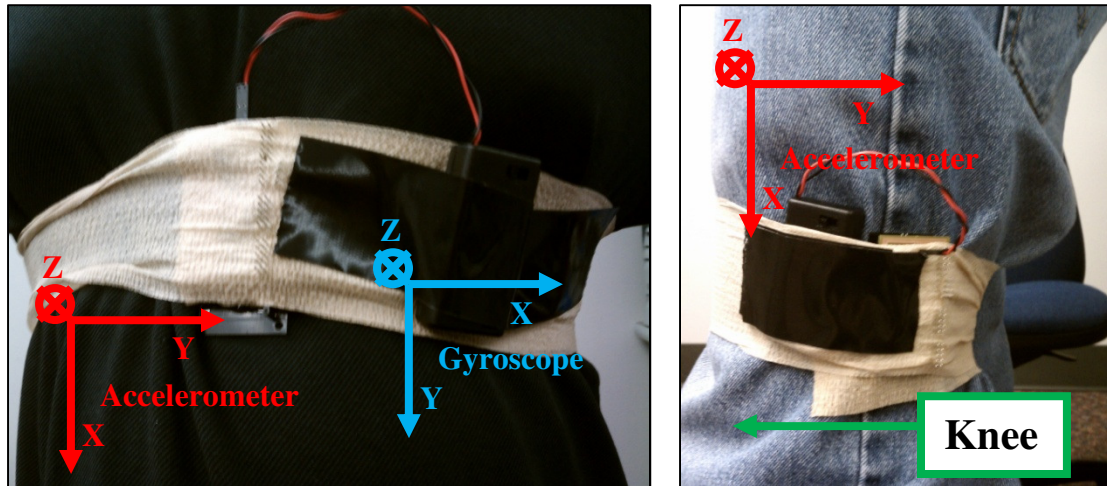
An additional useful feature of this program is its ability to be used on any platform. Although, the graphical interface will only work in Microsoft Windows, the data collection and ".csv" creation will work on any operating system. This portion of the program can be launched and controlled from the system's command line without the need for any graphical interface.

CHAPTER 6: RESULTS

The hardware and software/firmware discussed in Chapters 4 and 5 has been vigorously tested. The performance of each system was evaluated and the results are outlined in this chapter. It should be noted that the tests performed were designed to verify the functionality of the individual systems. The design was created such that each sensor system (i.e. Micro PAD, environmental system, and pulse oximeter) can be used simultaneously to collect data and find correlations. Although such an analysis is possible, the data collected has not been correlated to determine possible relationships as this would be outside the scope of the current research.

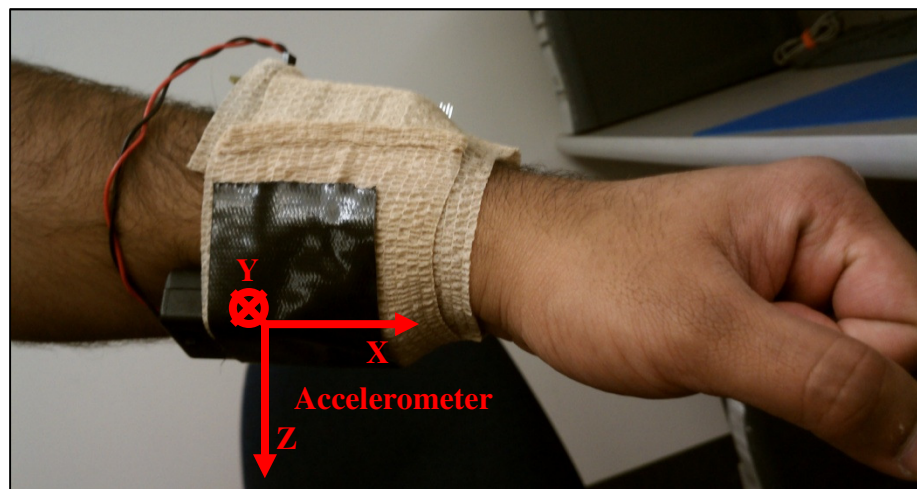
6.1 Micro PAD

Multiple tests were performed on the Micro PAD in order to prove its viability for physical activity tracking. For all tests, the accelerometers were oriented such that their X-axis was in the vertical direction when the test subject was standing upright with arms straight at their sides. The gyroscopes for each node were oriented such that their Y-axis was in the vertical direction for the same given body position (refer to Figure 3.1 for exact placements). Figure 6.1 shows the three nodes and their axis orientations. In order to improve the quality of the results and to show that the current system could be used for the various research applications, the quantity and placement of the sensor nodes for each test was determined by examining the published works of the research teams discussed in Chapter 2. Using their findings not only allowed for more meaningful results but also proved the ability of the current system to be used in multiple research applications.



(a) Chest Node

(b) Leg Node



(c) Arm Node

Figure 6.1: Micro PAD Node Placements and Sensor Axis Orientations

Multiple tests were completed to verify the design, but three of these tests can be adequately used to show the system's capabilities. The first test (Test 1) was a short series of activities that involved one sensor node attached to the chest. The test activities were sitting, standing, bending, walking, and running. The accelerometer was the only active device for this test. Figure 6.2 shows a graph of all data collected for Test 1. Varying accelerations along the different axes can be clearly seen for the activities performed

throughout the test. The next test of interest (Test 2) was a longer series of activities involving multiple active sensor types on three nodes. The node on the chest remained in the same position it occupied in Test 1. Another node was placed on the right leg just above the knee. The third node was placed on the subject's right arm just above the wrist (refer to Figure 3.1 for exact placements). The parameters of the third test (Test 3) were identical to those of Test 2, but the researcher was not present for the test subject's activities. Test 3 was completed without the researcher having knowledge of any activities in order to establish the ability to determine activity based on data analysis alone. Subsequent tests were completed, and their results were found to support the data collected from Test 1 through 3. The following subsections discuss the results of each test.

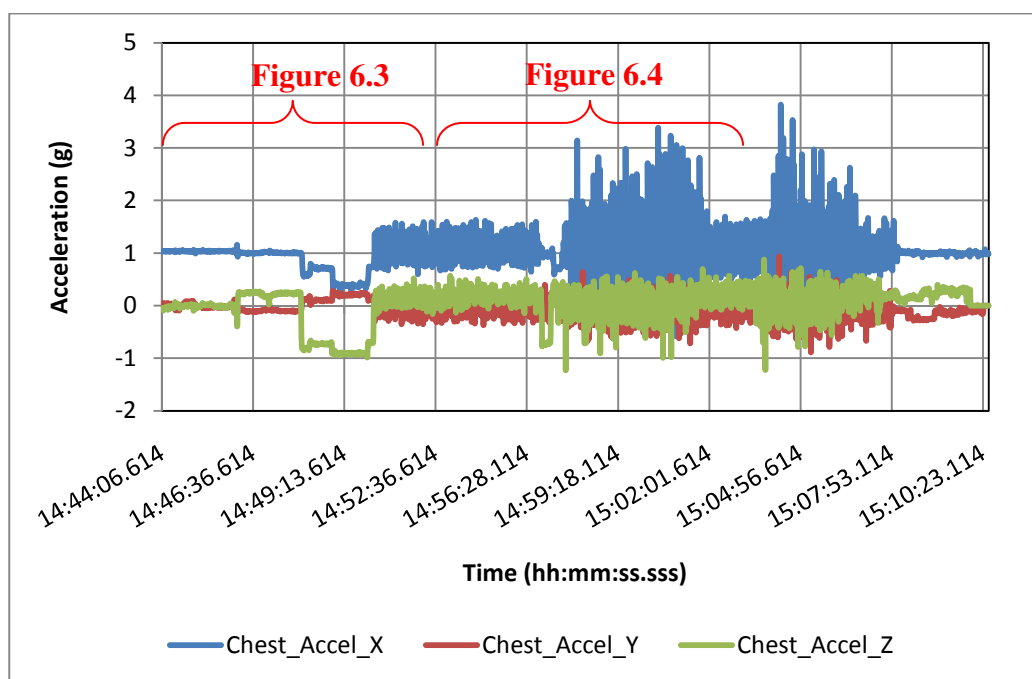


Figure 6.2: Test 1 Complete Activity Results for the Chest Accelerometer

6.1.1 Test 1 Analysis

Figure 6.3 depicts the results from the first series of test activities. The test subject started in a sitting position. This is shown as the relatively flat lines on all axes. Notice that the X-axis acceleration is at 1g. Different orientations of the sensor have set constant values on each axis. A constant value of 1g on the X-axis chest unit is indicative of either a sitting or standing position. At approximately 14:46:13, the subject stood. This can be seen as a sudden increase in acceleration in both the X and Z axes caused by the movement of the chest upward and forward (respectively). While standing, the subject favored one foot or the other swapping between the two as comfort dictated. This caused the non-zero values of the Y and Z axes. Then, the subject performed a series of bends at 14:48:03 of varying intensities. This is shown in the negative value for acceleration on the Z-axis and a diminished X-axis value. Lying down flat would have completely zeroed the Y and X-axes values. Finally, the end of Figure 6.3 shows some of the results from walking. During the walking process, the body moves up and down repeatedly, resulting in significant accelerations along the X-axis. Each step should cause one major upward spike and one downward spike in the data corresponding to a push-up with one leg and a bending of the leg as the foot returns to the ground (respectively). Consequently, more spikes in a given length of time would be indicative of a faster pace.

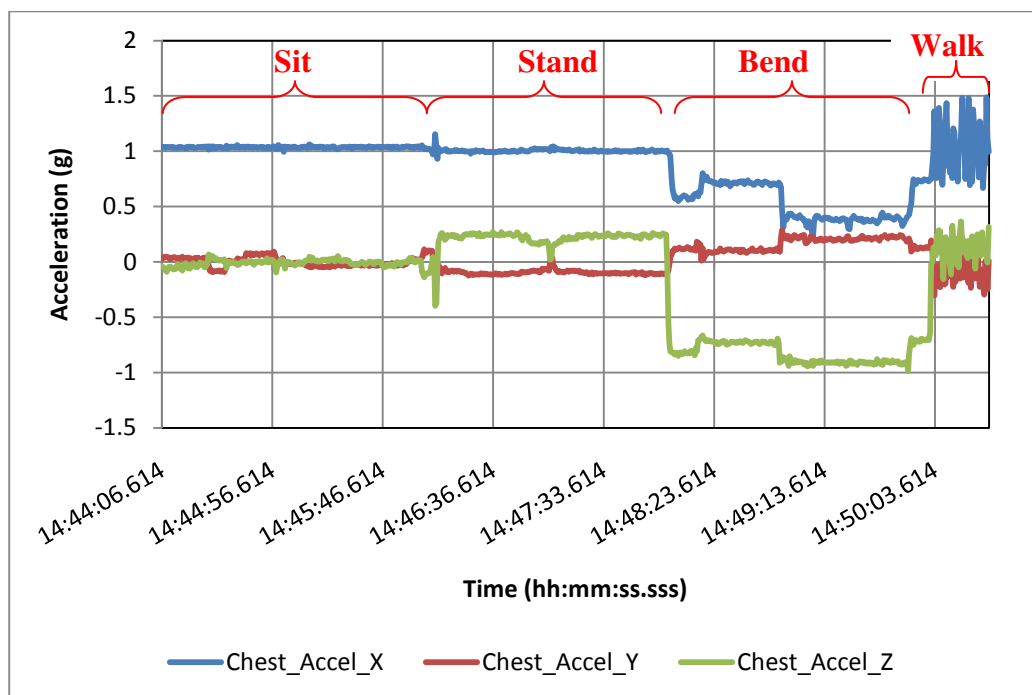


Figure 6.3: Test 1 Sit, Stand, Bend, and Walk Results for the Chest Accelerometer

Figure 6.4 shows a clear comparison between walking and running data. The walking data (14:50:34-14:57:00) is followed by a brief pause and bend for recording data (14:57:04-14:57:38). The next piece of data is a brief walk to a suitable test area followed by a 4 minute run at 14:57:42. The walk, stop, and bend activities are shown just as they were in Figure 6.3. The new data is the running activity. Notice that the accelerations during the run have greater magnitude across all three axes, but this is especially true for the X-axis. Running involves far more vertical motion because there is more bending of the knees and more of a push off the ground. Consequently, the X-axis of the accelerometer experiences more acceleration during a running activity than a walking activity. Furthermore, as discussed for the walking data, the pace of the test subject during a running activity can still be determined by the number of acceleration spikes in a given time period.

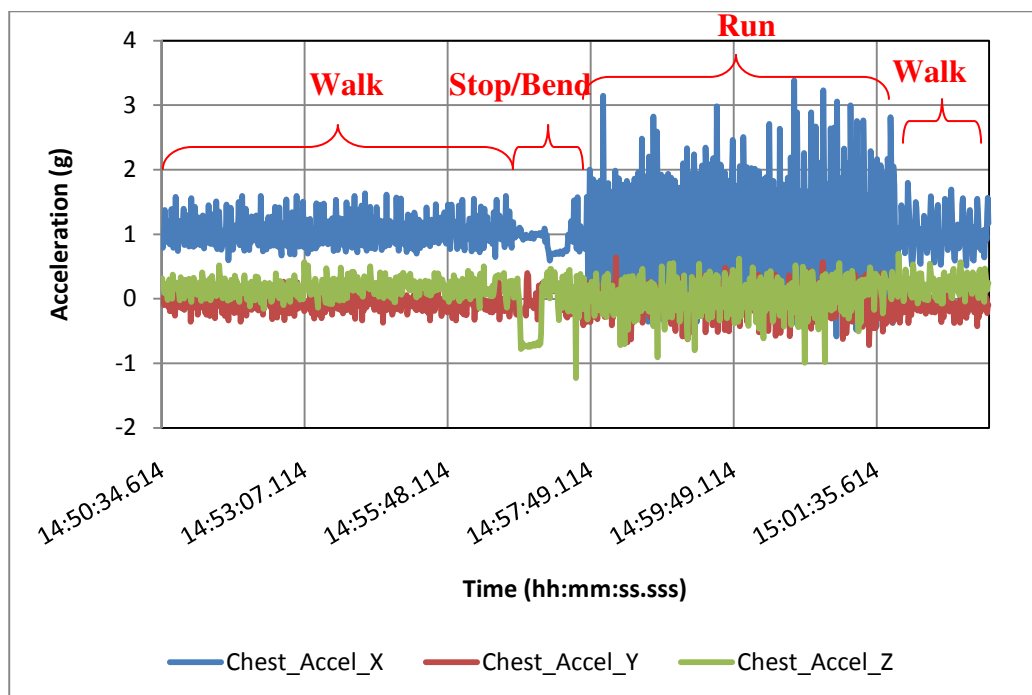
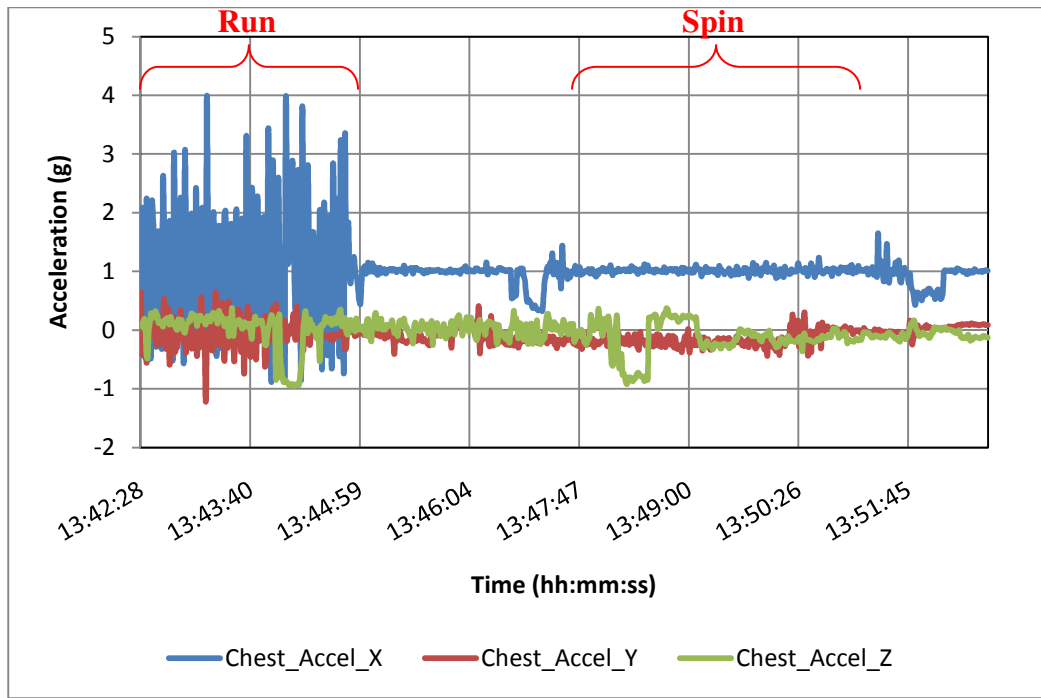


Figure 6.4: Test 1 Walk and Run Results for the Chest Accelerometer

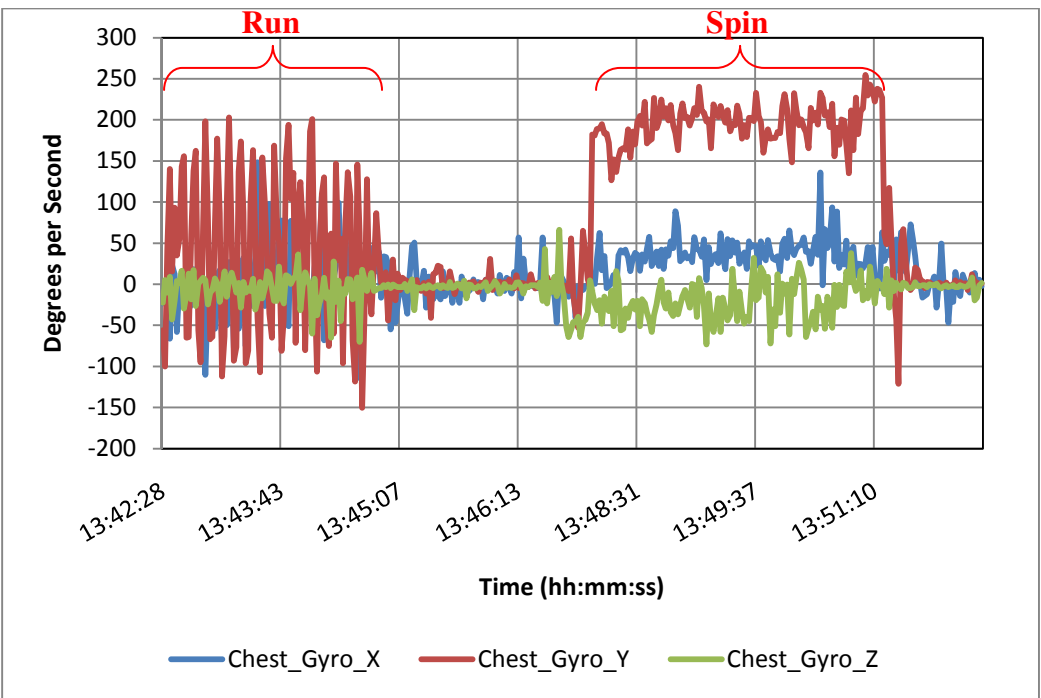
6.1.2 Test 2 Analysis

As shown in the previous results, a single accelerometer sensor placed on the chest can be used to determine a variety of activities. Data collected has been used to easily differentiate not only between stationary and active periods but also between different intensities of active periods (e.g., walking versus running). Such findings raise questions about the need for multiple sensor types on the same node. Consider a scenario in which a test subject is sitting in one spot but rotating (e.g., adjusting the seat to view another part of the desk). The data collected from an accelerometer placed on the subject's chest would collect data very similar to what is seen in Figure 6.5(a) from 13:47:30 to 13:51:07. All that can be determined from this data is that the test subject was either sitting or standing in one place. If, however, a gyroscope is present on that same sensor node, the collected data clearly shows the subject's change in angular acceleration

while rotating in a chair. Notice the increased acceleration on the Y-axis in Figure 6.5(b) for the same time range mentioned for Figure 6.5(a). This data was taken concurrently with the accelerometer data and gives the researcher a more complete view of the test subject's movements. Furthermore, consider the running activity discussed previously. The data collected from an accelerometer would be similar to that shown in Figure 6.5(a) from 13:42:28 to 13:45:00. This data indicates that the subject was running, but this is not the complete picture. For this particular test, the subject was confined to a small area in which to run. Thus, the path of motion was an elongated oval. Check the same time period for Figure 6.5(b), and notice the spikes in angular acceleration along the Y-axis. These spikes in acceleration occur every 1 to 2 seconds. This is approximately equal to the time it took the subject to run from one side of the room to the other. At which point, the subject would have to turn their body to run in the opposite direction, thus changing the acceleration on the Y-axis of the gyroscope for a brief period of time. Without the data from the gyroscope, nothing would indicate that the subject ever changed direction. This further shows that multiple sensor types on a single node can provide researchers with a more complete understanding of motion than a single sensor type.



(a) Chest Accelerometer

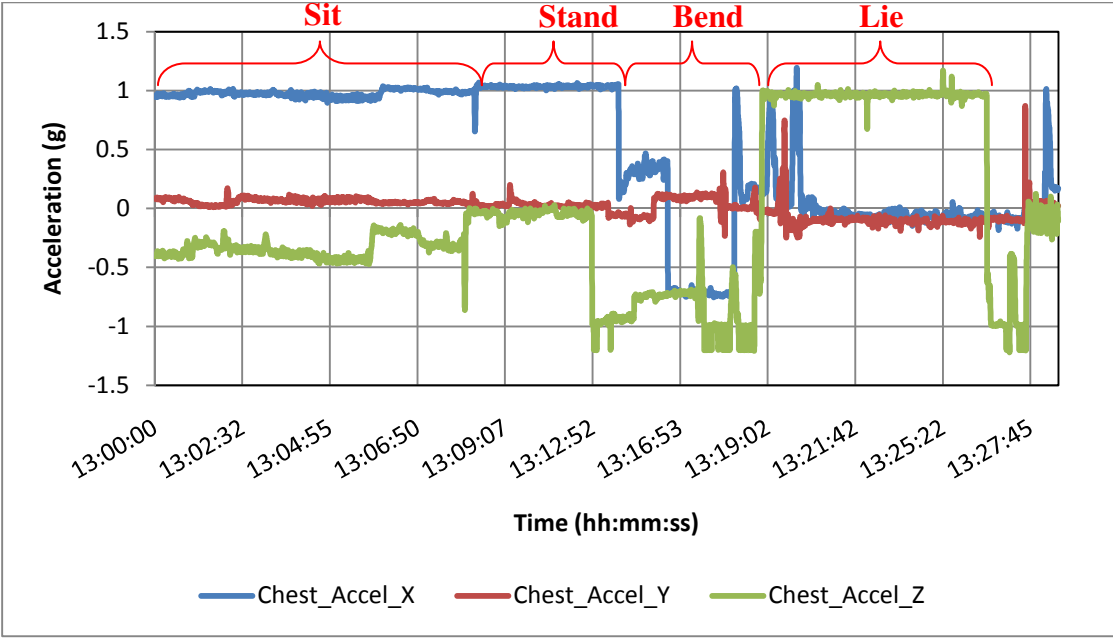


(b) Chest Gyroscope

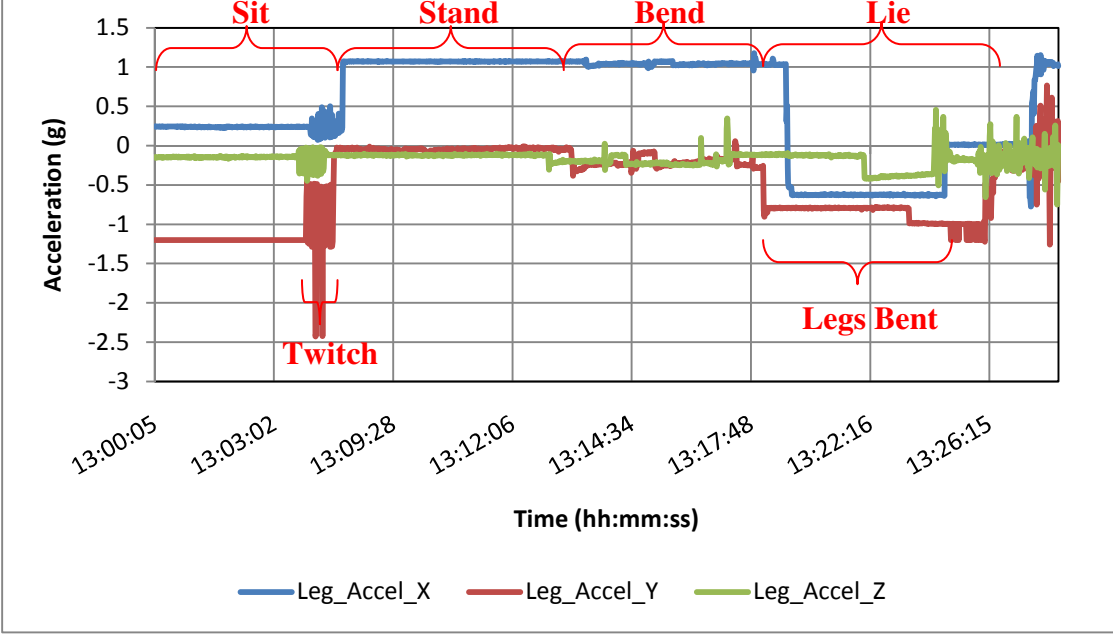
Figure 6.5: Test 2 Run and Spin Results for Chest Gyroscope and Accelerometer

All of the data discussed thus far has been collected from a single sensor node located on the test subject's chest. This setup has provided useful information on physical activity tracking as predicted by several of the research teams discussed in Chapter 2. While the data collected has provided a fairly accurate picture of the subject's movements, it has by no means described every movement made by the test subject. As previously stated, multiple sensor nodes attached at different points of the body must be used in order to fully track a person's movement. As proof of this statement's validity, examine the data from Figure 6.6(a) from 13:00:00 to 13:20:00. This data, provided by a sensor node placed on the chest as in Figure 6.3, shows nothing more than a test subject either standing or sitting. Differentiation between the two positions is impossible to determine from this data alone. At approximately 13:08:00, the test subject stood upright. Notice the changes in acceleration that take place in Figure 6.6(b) at this time. The Y-axis acceleration changes from -1g to 0g and the X-axis acceleration increases from around 0g to 1g. This tells the researcher that the subject's upper leg is now perpendicular to the floor rather than parallel. Thus, the sensor node attached to the leg has shown the test subject to be in a standing position. Additionally, the chest sensor still shows an upright position of the torso. Therefore, the data from the two nodes has accurately shown that the test subject was standing upright. The difference between standing upright and standing while bent to varying degrees can be seen in the acceleration changes of the chest unit in Figure 6.6(a) from 13:13:30 to 13:18:55. Another benefit of the leg sensor is the ability to record activity in the lower extremities while a subject's trunk remains stationary. This is shown from 13:03:30 to 13:08:00 in Figure 6.6(b). During this time, the test subject's leg was twitching nervously up and down. This was picked up by the leg

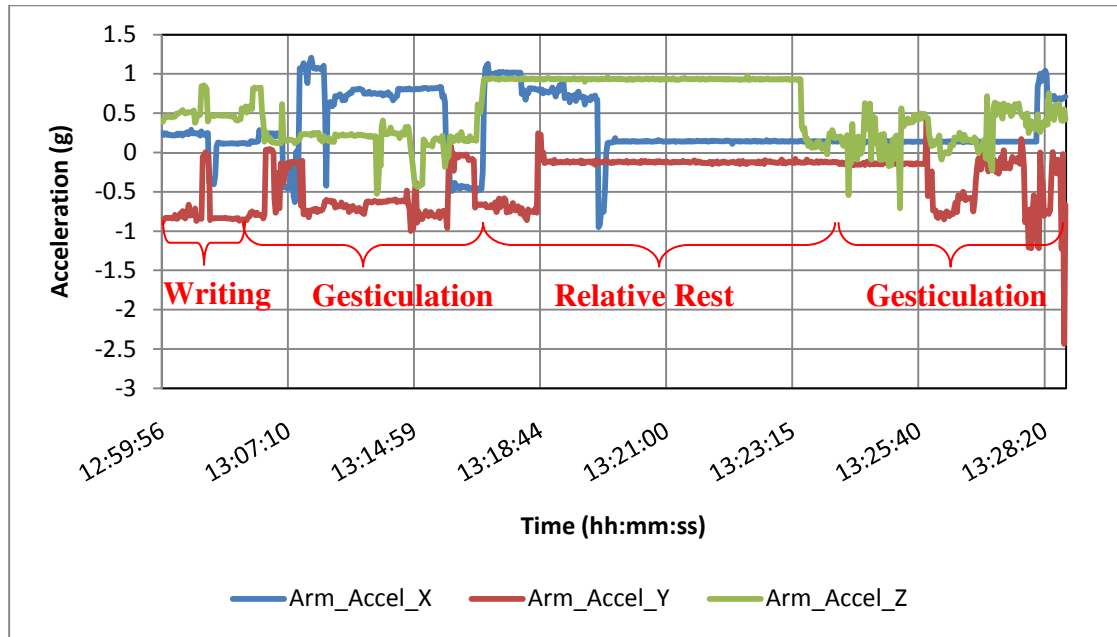
node's accelerometer as fluctuations along its Y-axis. Another example of this can be seen while the test subject was lying down (indicated by the chest unit's 1g Z-axis reading) between 13:20:00 and 13:28:00. Until 13:25:00, the leg accelerometer was reading between -0.5 to -1g on the Y and X-axes. This indicates that the sensor was oriented such that these two axes were positioned at around a 45-60 degree angle with respect to the floor. Thus, the subject's leg was at an incline while they rested. The sensor node located on the arm also provided useful information on the subject's stationary activities. A glance at Figure 6.6(c) from 12:59:56 to 13:20:00 will show that the subject's arm was quite active throughout this portion of the test. Analysis of this data could give the precise orientations of the arm and possibly distinguish the exact activity in which the subject was engaged. The data up to 13:03:30 shows that the sensor's Y-axis was basically perpendicular to the ground with consistent activity along the Z-axis and occasional spikes of acceleration in the other two axes. From this, it can be concluded that the subject's arm was parallel to the ground with their thumb pointing upward, and their hand was moving mostly from side to side with occasional movements back and forth. This could be indicative of a number of activities ranging from gesticulation to writing (as was the case in this instance).



(a) Chest Accelerometer



(b) Leg Accelerometer

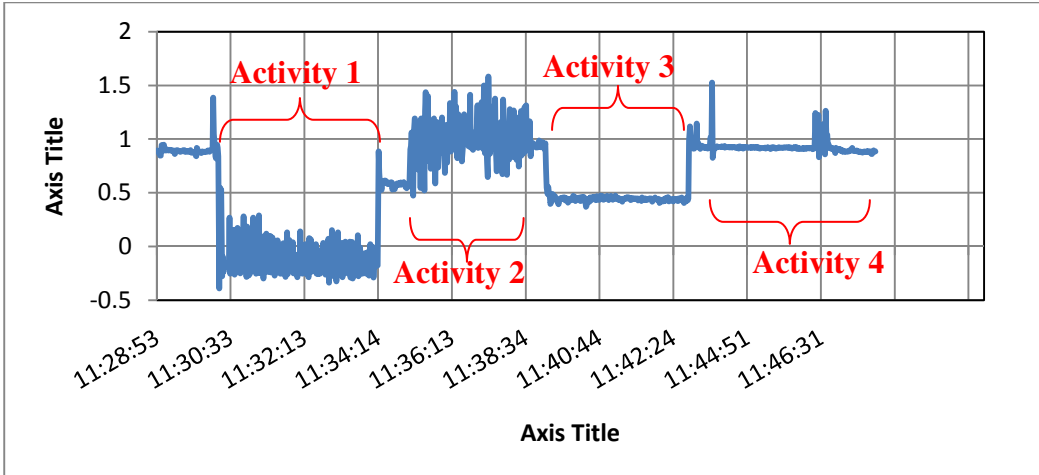


(c) Arm Accelerometer

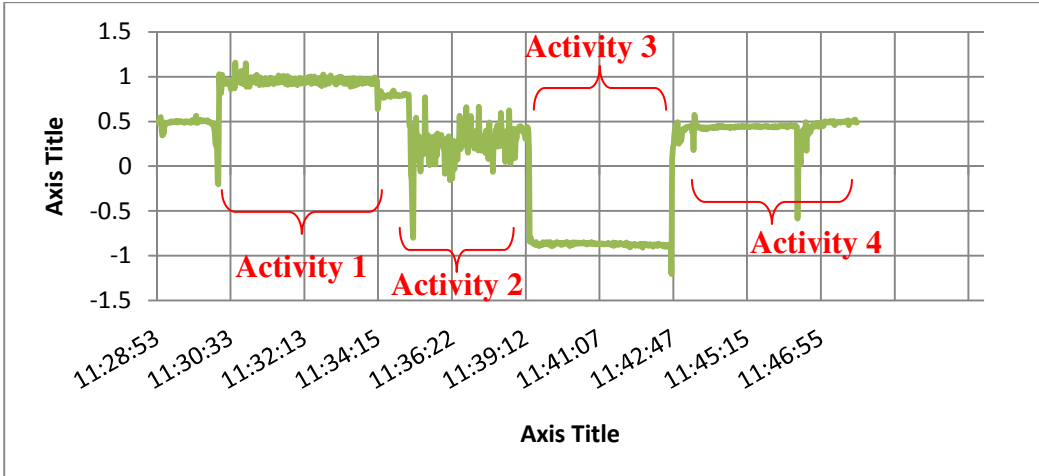
Figure 6.6: Test 2 Stationary Activity Results for Chest, Arm, and Leg Accelerometers

6.1.3 Test 3 Analysis

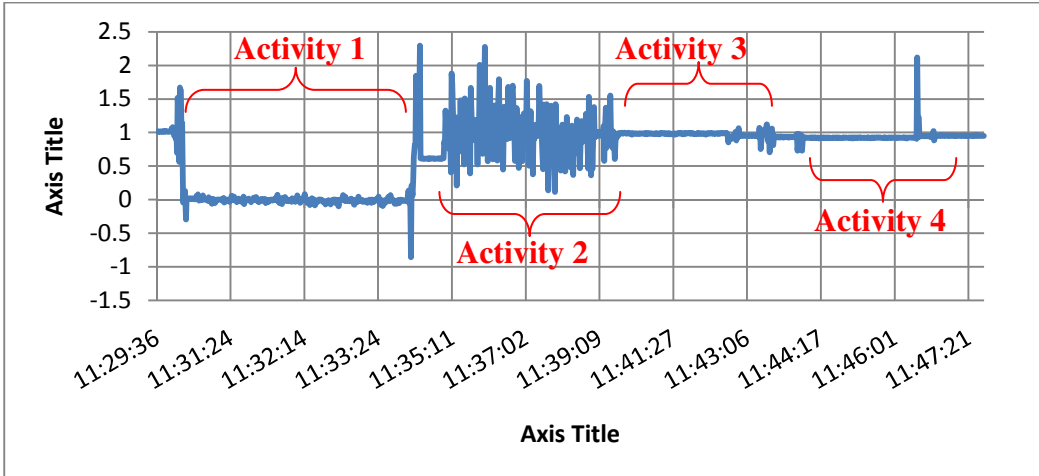
The results from the previous two tests prove that the Micro PAD design is capable of producing stable results that can be analyzed to reconstruct a person's body positions and movements. However, they do not confirm the ability to determine physical activity without prior knowledge of a subject's movements. Thus, the test subject was told to choose a series of 4 random activities for Test 3 and keep them secret until after the researcher finished the post-experiment analysis. At this point, the researcher left the room, the activities were completed, and the collected data was analyzed as shown in the previous two subsections. The inclusion of all data collected for this test would be overwhelming. Therefore, only portions of particular interest are depicted in Figure 6.7.



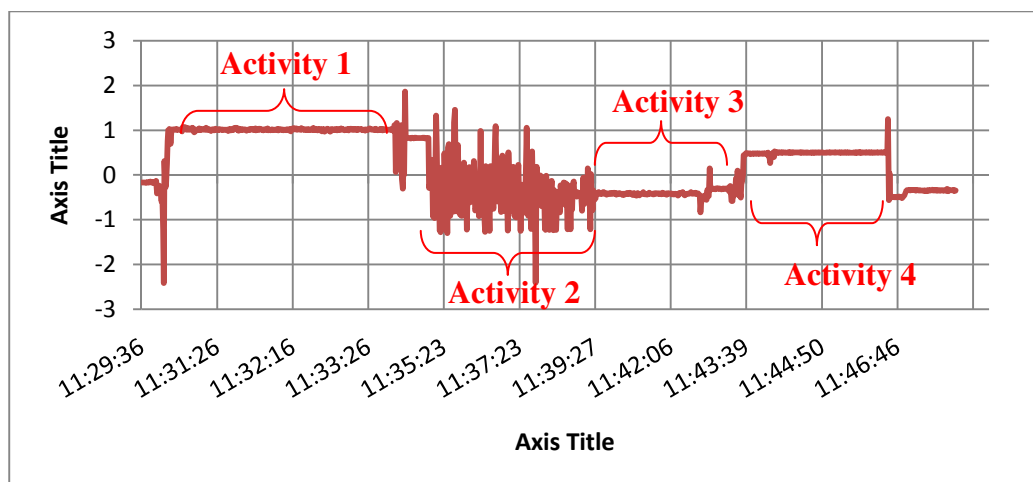
(a) Chest Accelerometer X-axis



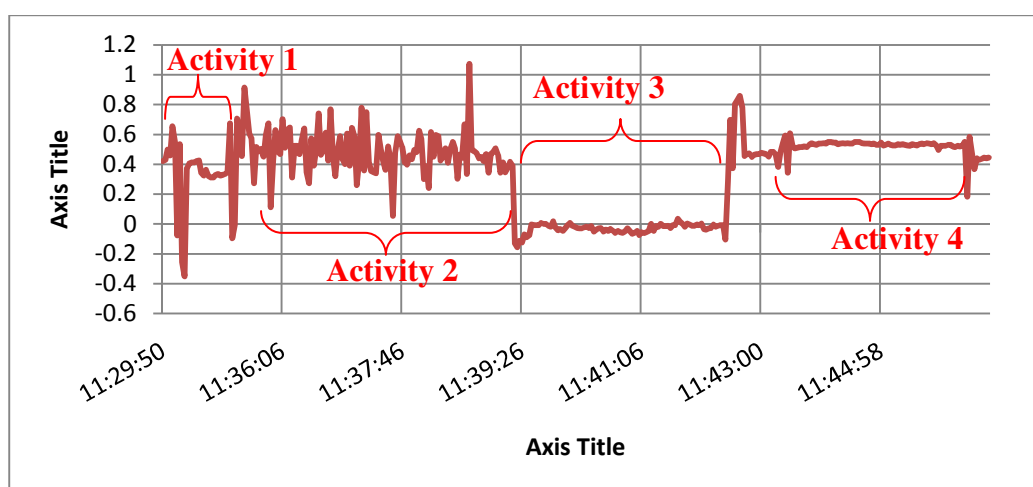
(b) Chest Accelerometer Z-axis



(c) Leg Accelerometer X-axis



(d) Leg Accelerometer Y-axis



(e) Arm Accelerometer Y-axis

Figure 6.7: Test 3 Data for Unknown Activities Performed by Test Subject

With the exception of a few minor glitches in data, the results of the analysis provided an accurate description of the subject's activities. The first activity (Activity 1 in Figure 6.7) selected by the test subject was sit-ups. The results of the analysis showed the subject lying down with regular movements of the torso up and down (see Figure 6.7(a) and Figure 6.7(b)). This being consistent with sit-ups, the researcher correctly guessed the activity. The only mistake in the analysis was with respect to the leg position. The data clearly shows that the subject's upper leg was parallel to the ground (see Figure

6.7(c) and Figure 6.7(d)) indicating that the legs were flat. However, the subject claimed that the leg was bent in the standard sit-up position. The second activity was a brisk walk. Using the methods of analysis described in the previous subsections, the researcher was able to determine not only that the subject was walking quickly (see Figure 6.7(a)) but also that their arm was swinging back and forth (see Figure 6.7(e)). The third activity was a stationary 90 degree bend at the waist (see Figure 6.7(b) and Figure 6.7(c)) with arms hanging down perpendicular to the ground. The researcher was able to get every aspect of this activity perfectly correct. The final activity was a simple sitting position with the arm on an armrest. Similarly to the first activity, the researcher got everything correct except for the leg position. This time, the data clearly showed the subject in a standing position (see Figure 6.7(a) and Figure 6.7(c)). The incorrect data on the leg sensor for these tests were most likely caused by improper positioning of the leg sensor or an unwanted shift in the placement of the device. Thus, the majority of the analysis was correct and the results show that activities can be judged fairly accurately without previous knowledge.

6.2 Pulse Oximeter

The pulse oximeter design has been tested and improved extensively for months. Issues pertaining to stability and reliability appear to have been fixed and the system is providing adequate results for the current research. These results can be seen most clearly in Figures 5.5(b) and 6.8. The output of the receive circuit (Figure 5.5(b)) provides the microcontroller with an accurate heartbeat signal ranging in amplitude from 20 to a few hundred mV_{pp} depending on the location of the sensor and the strength of the test subject's pulse. This allows the microcontroller to calculate the subject's heartbeat to within ± 5 bpm of commercially available pulse oximeters. The system still experiences a

loss of signal given severe movement of the sensor, but analysis of other commercial devices and research completed in [4] and [6] has shown that this error is an expected problem with this technology.

After the calculations have been completed, the data is ready to be stored and/or displayed. The MiFOXI can send data via its UART port to be displayed on a HyperTerminal program (see Figure 6.8), or it can be transmitted to the on-board Zigbit. The radio will then send the data to its base node for further processing or storage on a secure digital (SD) card. Once stored, the SpO₂ and pulse data can be compared to results stored by the environmental and physical activity monitoring systems.

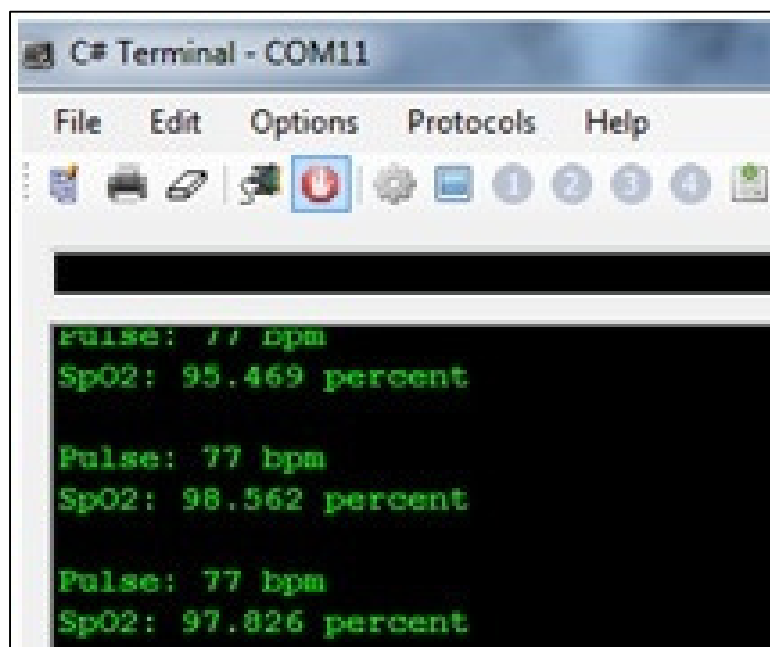
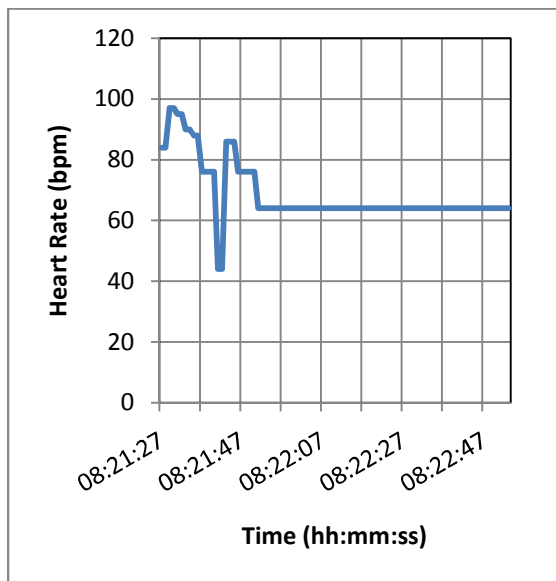


Figure 6.8: SpO₂ and Pulse Data Displayed on a HyperTerminal

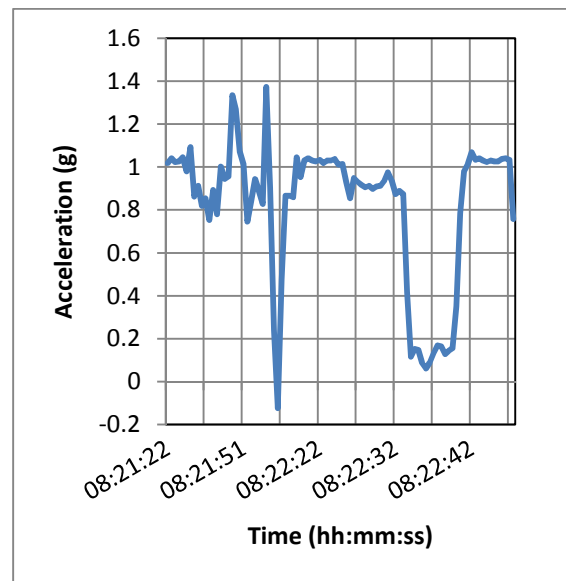
The final series of tests conducted on the MiFOXI Daughter design were completed in order to confirm its functionality on the Fusion network. The parameters of these experiments were simple. The Micro PAD systems were attached to the test subject

as described in the previous sections along with a single MiFOXI Daughter. Additionally, a Fusion board with humidity and temperature sensors was included to provide a more complete representation of sensors. All sensor nodes were wirelessly connected to a base node (Fusion board) and the data was collected for a few activities.

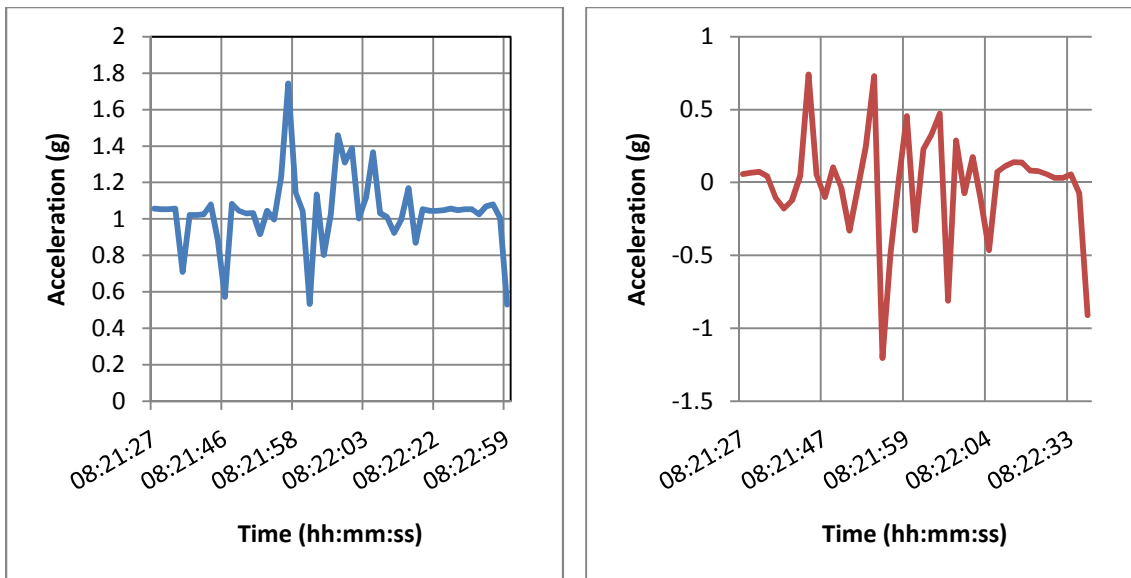
The first activity was a simple resting position. The test subject stood and completed minor tasks at a desk. This can be clearly seen in Figure 6.9(b) through Figure 6.9(d). The accelerations shown on the axes for the chest and leg accelerometers show that the torso and upper leg were mostly vertical (see Section 6.1 for full analysis). The random spikes of data are easily attributed to movement caused by the various activities completed while in the sitting position. Figure 6.9(a) shows the subject's heart rate for the duration of this test. The elevated heart rate seen at the front of the test was determined to be a result of the subject's excitement from completing a difficult task. The subject regained their composure and the rest of the data shows a more stable heart rate (approximately 64 bpm).



(a) Pulse Oximeter



(b) Chest Accelerometer X-axis

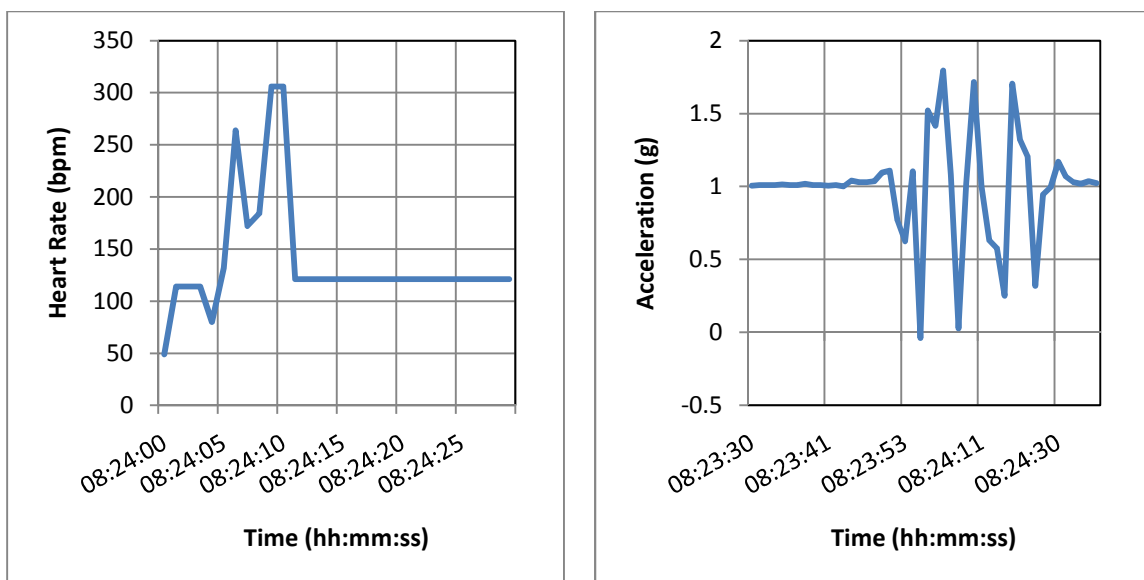


(c) Leg Accelerometer X-axis

(d) Leg Accelerometer Y-axis

Figure 6.9: First Rest Activity Data for Accelerometers and Pulse Oximeter

The second activity was designed to elevate the test subject's heart rate by means of physical exertion. The subject was asked to jog for a short period of time. This can be seen by the spikes of data in the X-axis of the chest accelerometer shown in Figure 6.10(b). Notice the heart rate in Figure 6.10(a) increases from 50 bpm to just over 100 bpm shortly after the test subject started their run. The next set of spikes from 8:24:04 to 8:24:12 were caused by the jarring of an improperly secured MiFOXI Daughter, but the rest of the data shows a clearly elevated heart rate (121 bpm) as compared to the resting heart rate of Figure 6.9(a).

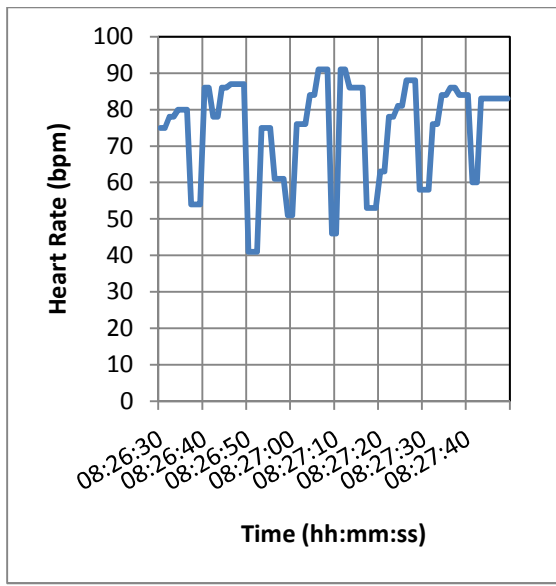


(a) Pulse Oximeter

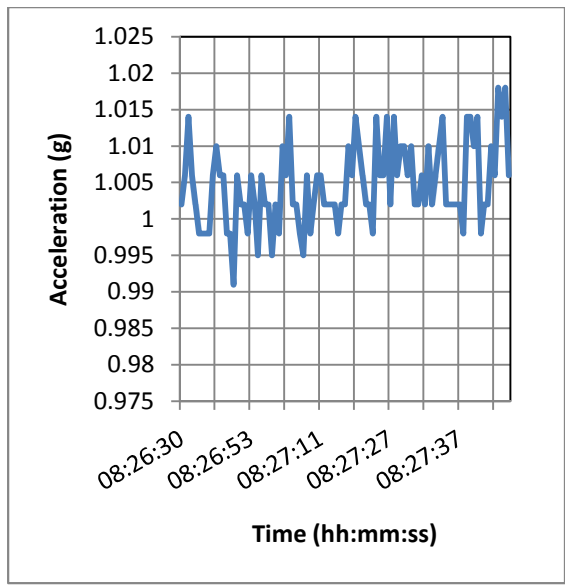
(b) Chest Accelerometer X-axis

Figure 6.10: Running Activity Data for Chest Accelerometer and Pulse Oximeter

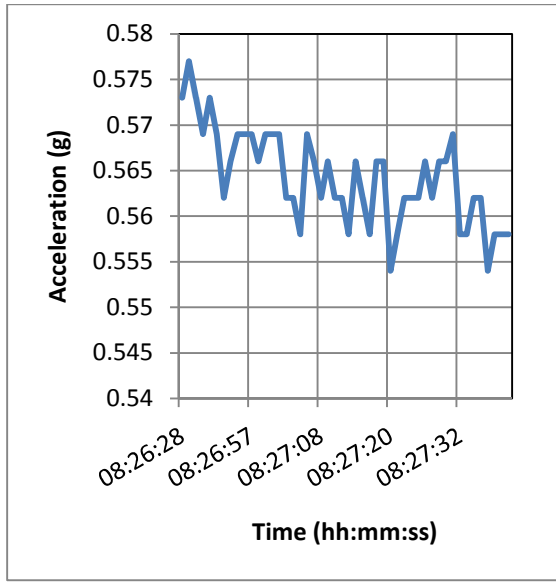
The final set of tests were designed to show fluctuations in heart rate without the presence of physical strain. The test subject was asked to try various stationary activities to modify their heart rate (e.g., increase respiration, concentrate on a stressful thought, etc.) while sitting in a chair. The results of the attempt at altering their heart rate can be seen in Figure 6.11(a). It should be noted that the spikes below 50 bpm should be ignored as they were caused by faulty calculations for the individual's heart rate. Figure 6.11(b) through (c) show the subject's sitting position. The near -1g acceleration on the Y-axis of the leg accelerometer indicates a mainly horizontal positioning of the upper leg, and the 1g value on the X-axis of the chest accelerometer is indicative of a vertical torso. The non-zero value on the X-axis of the leg accelerometer that shows the subject's upper leg was at a slight angle was due to their position in the chair. The subject was sitting on the edge of the chair with their feet behind them and their knees lowered.



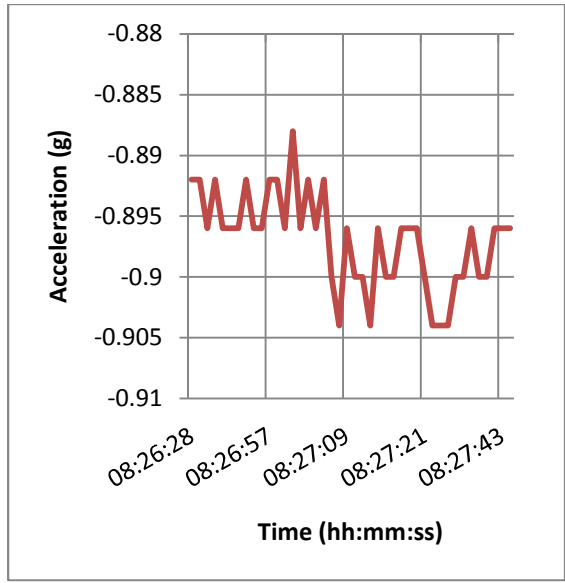
(a) Pulse Oximeter



(b) Chest Accelerometer X-axis



(c) Leg Accelerometer X-axis



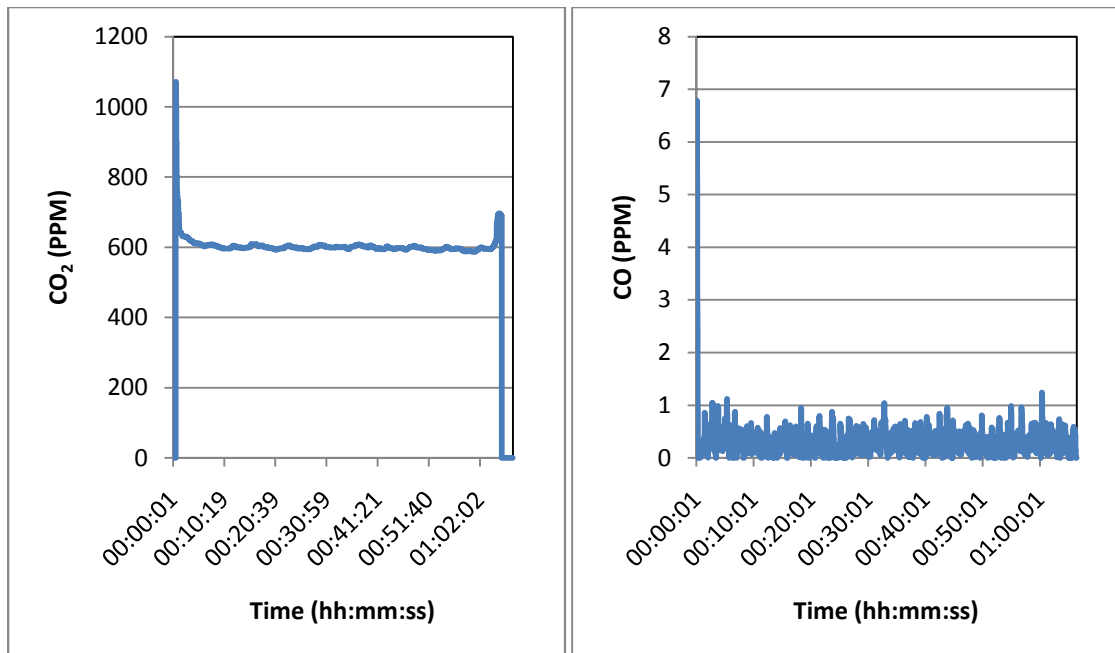
(d) Leg Accelerometer Y-axis

Figure 6.11: Second Rest Activity Data for Accelerometers and Pulse Oximeter

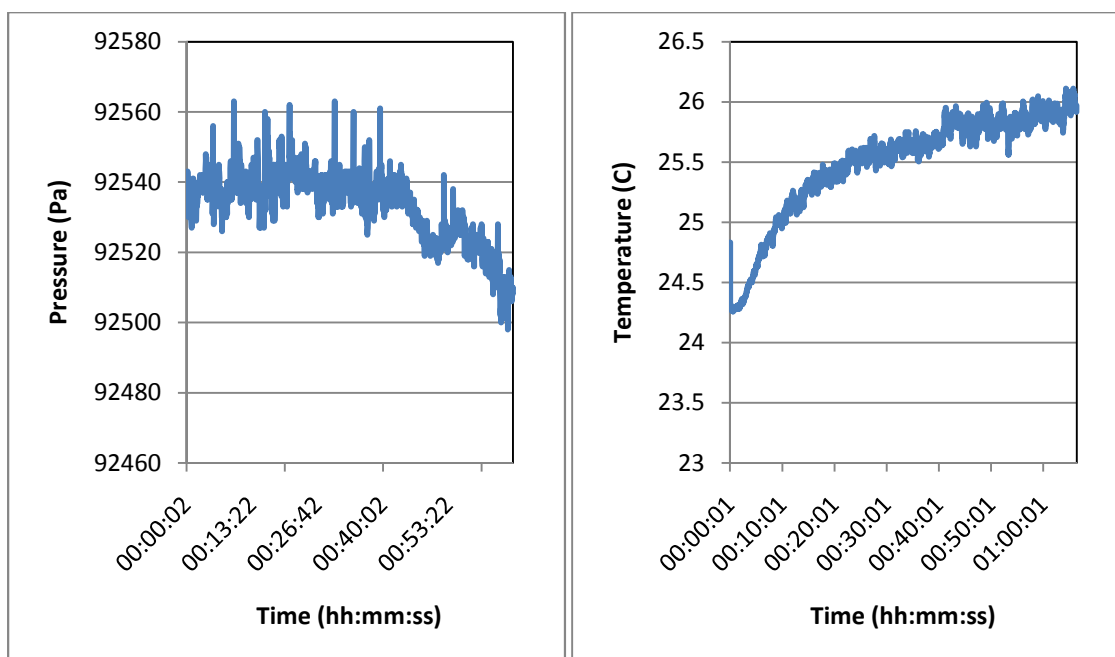
6.3 Environmental Sensor Daughterboards

The environmental sensing system performs to specification. More specifically, the Fusion motherboard is capable of collecting and processing data from sensors connected via daughterboards. Multiple daughterboards have been and continue to be

designed. Operation of the firmware for all of the available low level communication protocols has been verified. Integrating new sensors is now as simple as building a daughterboard and writing the sensor specific drivers. As they are created, daughterboards are tested extensively and potential sources of data collection errors are resolved. Examples of collected data can be seen in Figure 6.12. The data displayed in the graphs came from multiple daughterboards (as discussed in Section 4.3). Information can be collected on the various environmental factors simultaneously with the physical activity and pulse oximeter data. Then, it can be correlated to determine possible relationships.

(a) CO₂ Data

(b) CO Data



(c) Atmospheric Pressure Data

(d) Temperature Data

Figure 6.12: Environmental Sensor Data

CHAPTER 7: CONCLUSIONS AND FUTURE WORK

The current research has been successful in the design and implementation of a flexible system for use in a wide range of physical activity tracking applications. The goals set forth in Chapter 1 have been met and the current design has been proven to be capable of physical activity tracking, environmental conditions monitoring, and certain types of biomedical sensing. Although the design is not without areas in need of improvement, it is fully capable of meeting the needs of the current research. The following sections offer some conclusions and suggestions for future work for the various aspects of the design.

7.1 Personal Sensor Network

The implementation of the WPSN is a major part of the success of the current research. The wireless design allowed for easier testing and reconfiguration of sensing system for the various test procedures. In addition to making the testing process simpler, the wireless network also adds considerably to the flexibility of the entire system. Adding and subtracting nodes in the network only requires the researcher to turn a programmed device on or off. Thus, different tests may easily be conducted with a variable number of sensors connected to different parts of the body or environment without the need for hardware modifications or reprogramming nodes. As the design stands, the network is more than adequate for the needs of the current research and could be improved in only a few minor aspects. The implementation for the network only transmits data. The addition of a command interface that allowed researchers to turn nodes/sensors on/off remotely

and request data/identifiers from specific sensors would be very useful. Also, research into more efficient ways to transmit data could be highly beneficial by increasing data throughput. The current implementation transmits data in a string format. This makes transmissions easy to read without specialized software, but a simpler format (e.g., binary representation) could greatly decrease packet size for applications requiring higher throughput.

7.2 Micro PAD

The Micro PAD design functions very well as a physical activity tracking system. Even at low sampling frequencies (e.g., 1-2 Hz), the system can be accurately used to differentiate between a wide range of activities. For future studies, the creation of more nodes and Micro PAD boards could provide more interesting results. As shown in Section 6.1, the use of three nodes provided the researcher with a clearer picture of the test subject's movements. Adding more nodes to the network on different parts of the body could allow for the tracking of more subtle movements and a better determination of the body position/activity in which the test subject is engaged. Also, the additional information provided by the gyroscope in Section 6.1.2 proved useful for tracking physical activity. Thus, it may also be advantageous to add more sensor types for tracking motion (e.g., magnetometers, digital compasses, etc.).

Besides the previously discussed hardware additions, the firmware for the Micro PAD could also use more work. Due to time constraints, some of the modules for system resources on the Micro Fusion motherboard contain blocking code. The implementation of a completely non-blocking codebase would improve system performance by allowing for more data throughput and higher sample rates for the sensors.

7.3 Biomedical System

The pulse oximeter provides a fairly accurate heart rate measurement and a believable value for SpO_2 (calibration using specialized equipment is required for accurate measurements). After filtering the heartbeat signal, it appears clean and can easily be used for SpO_2 calculations and peak detection. The system appears to be stable and is capable of performing the desired tasks of indicating increased strain or change in blood oxygenation. That being said, this system is not devoid of areas that could use improvement.

First and foremost, the title given to this portion of the design is "Biomedical System." Although a pulse oximeter does fall under this category, it is not the only sensor that could be given such a title. The design should be expanded to include more sensors for monitoring other physiological responses (e.g., body temperature, respiration, perspiration, etc.). Additionally, other types of pulse sensing technology less prone to errors during extreme movement could be explored (e.g., electrocardiogram sensors). An oximeter may still be needed if SpO_2 measurements are required, but the second pulse sensing option may be useful to check the oximeter readings.

Secondly, as it currently stands, the pulse oximeter uses positive feedback for the transimpedance amplifier. Although the current design works, it seems to be very sensitive to sensor placement and experiences glitches (see Section 6.2). This has been largely attributed to the nature of biomedical sensing and the well known shortcomings of pulse oximetry with respect to movement. However, part of the instability could be the design of this first stage of amplification. The positive feedback is most likely adding noise into the output of the transimpedance amplifier. This could cause problems for the

digital DC tracking filter, which could result in the occasional loss of signal at the output of the second stage of amplification. Work has been started on a design that uses negative feedback to achieve the same output. Figure 7.1 shows the new schematic. Initial testing has shown that the new design produces comparable results to the system using positive feedback. However, further tests and adjustments of values will be required before the new design can be finalized. Additionally, according to [25], positive feedback in a photodiode transimpedance amplifier can be useful. However, the schematics depicting this implementation show positive feedback used in conjunction with negative feedback to provide the desired functionality. The current system was only tested with positive or negative feedback (not both). Thus, it would be interesting to redesign the system to incorporate both and compare performance. One final area of hardware redesign might include the development of an analog system to replace the digital DC tracking filter. This would remove all floating-point calculations and blocking SPI calls from the ISR and improve system stability.

Finally, the pulse oximeter code and hardware could use a few upgrades to improve the performance of the design. The current LED/photodiode probe is a rough prototype that could easily be replaced with a commercially available probe. This would eliminate mechanical errors from the system measurements. Additionally, the code for the design is very rough and only loosely follows the coding practices set forth in [13]. Cleaning up the code to meet these standards would greatly improve the readability/maintainability of the code and improve performance.

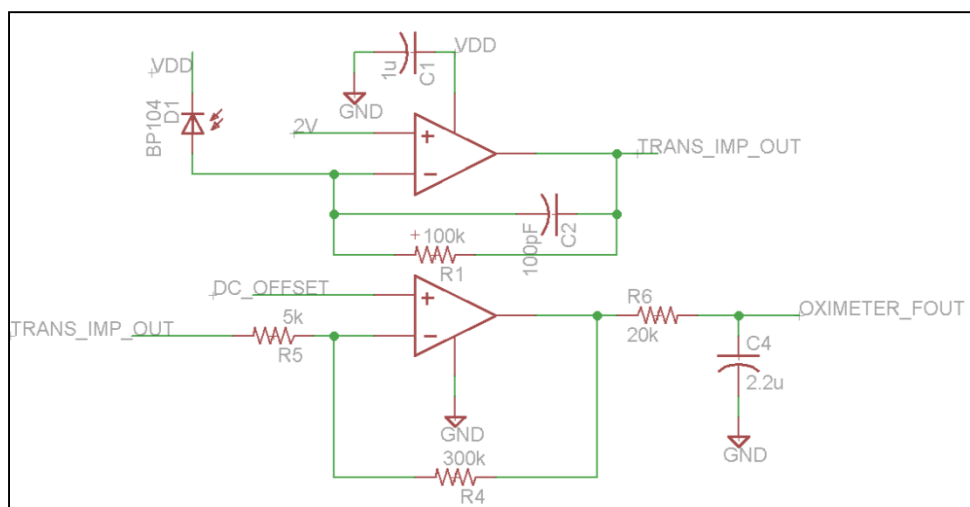


Figure 7.1: Redesigned Oximeter Receive Circuit

7.4 Environmental Sensing

Environmental sensing is a critical part of the current research. Tracking environmental conditions provides researchers with a clearer picture of a test subject's physiological response by allowing them to differentiate between response to physical activity and response to environmental stimuli. Although still in development, the environmental sensing system of the current design is more than capable of meeting the needs of this research. The system design is highly flexible and capable of accepting a wide variety of sensor technologies. The necessary future work for this system includes the creation of more daughterboards and the integration of new environmental sensors.

7.5 General Purpose Design

The primary goal of the current research was to design and create a flexible physical activity tracking system capable of collecting data on motion, physiological response, and environmental conditions. The developed system comprising two motherboards and a series of daughterboards for sensing such parameters has met these

specifications. Due to the careful consideration given to hardware and software development, the current system is highly reconfigurable with minimal design work. The Fusion and Micro Fusion motherboards can accept a wide range of sensors, and the implementation of a daughterboard system allows the various sensors to be swapped easily. Furthermore, the WPSN implementation gives the ability to add or subtract nodes from the system quickly without the need for hardware modifications or reprogramming of any part of the system. Any configuration of Fusion and Micro Fusion boards may be used in the system and attached to any part of the body. Thus, the system can be easily adjusted to work for the widest possible range of research applications.

REFERENCES

- [1] World Health Organization. "Electromagnetic Fields and Public Health: Base Stations and Wireless Technologies" World Health Organization Media Centre. World Health Organization. May 2006. Web. 7 Feb. 2011
- [2] Curone, D., Tognetti, A., Secco, E.L., Anania, G., Carbonaro, N., De Rossi, D., Magenes, G. "Heart Rate and Accelerometer Data Fusion for Activity Assessment of Rescuers During Emergency Interventions." *Information Technology in Biomedicine, IEEE Transactions on* 14.3 (2010): 702-710. Web. 2 Jan. 2011.
- [3] Wixted, A., Thiel, D., Hahn, A., Gore, C., Pyne, D., James, D. "Measurement of Energy Expenditure in Elite Athletes Using MEMS-Based Triaxial Accelerometers," *Sensors Journal, IEEE* 7.4 (2007): 481-488. Web. 2 Jan. 2011.
- [4] West, J. B. *Pulmonary Pathophysiology: The Essentials*. Williams & Wilkins, 2003. Web. 15 October 2010.
- [5] Mayo Clinic Staff. "Hypoxemia (Low Blood Oxygen)" Definition. Mayo Clinic. Sept. 2010. Web. 17 Nov. 2010
- [6] Severinghaus, J. and Honda, Y. *History of Blood Gas Analysis: VII. Pulse Oximetry*. J Clin Monit, 1987. Web. 10 October 2010.
- [7] Matviyenko, S. "Application Note AN2313: Pulse Oximeter." Cypress Semiconductor Corporation. 2005. Web. 1 Sept. 2010.
- [8] Chan, V. and Underwood, S. "A Single-Chip Pulsoximeter Design Using the MSP430." Texas Instruments. June 2010. Web. 1 Sept. 2010.
- [9] Grap, M. (2002). "Pulse Oximetry." *Critical Care Nurse*. 22.3 (2011): 69-74. Web. 16 Jan. 2011
- [10] Respir Care. "AARC Clinical Practice Guideline: Pulse Oximetry." *AARC and Respiratory Care Journal* 1.1 (1992): 37(8), 891-897. Web. 7 Nov. 2010.
- [11] LeMura, L. & Duvillard, S. *Clinical Exercise Physiology: Application and Physiological Principals*. Philadelphia: Lippincott Williams & Wilkins, 2004. Web. 2 Feb. 2011.

- [12] Johns Hopkins Medical Institutions. "Inability To Pump Oxygen During Exercise Could Pinpoint Early Heart Problems." *ScienceDaily*. October 2003. Web. 7 February 2011
- [13] Pook, M., Loo, S. M., Planting, A., Kiepert, J., & Klein, D. (2010). "Coding Practices for Embedded Systems," *2010 ASEE Annual Conference* 10.1 (2010). Print.
- [14] Khan, A.M., Young-Koo L., Lee, S.Y., Tae-Seong, K. "A Triaxial Accelerometer-Based Physical-Activity Recognition via Augmented-Signal Features and a Hierarchical Recognizer," *Information Technology in Biomedicine, IEEE Transactions* 14.5 (2010): 1166-1172. Web. 2 Jan. 2011.
- [15] Bouten, C.V.C., Koekkoek, K.T.M., Verduin, M., Kodde, R., Janssen, J.D. "A triaxial accelerometer and portable data processing unit for the assessment of daily physical activity," *Biomedical Engineering, IEEE Transactions on* 44.3 (1997): 136-147. Web. 2 Jan. 2011.
- [16] Tseng, Y., Wu, C., Wu, F., Huang, C., King, C., Lin, C., Sheu, J., Chen, C., Lo, C., Yang, C., Deng, C. "A Wireless Human Motion Capturing System for Home Rehabilitation," *Mobile Data Management: Systems, Services and Middleware, International Conference on* 1.1 (2009): 359-360. Web. 2 Jan. 2011.
- [17] Wu, J., Dong, L., Xiao, W. "Real-time Physical Activity Classification and Tracking Using Wearable Sensors," *Information, Communications & Signal Processing, 2007 6th International Conference on* 1.1 (2007): 1-6, 10-13. Web. 2 Jan. 2011.
- [18] Dong, L., Wu, J., Chen, X. "Real-time Physical Activity Monitoring by Data Fusion in Body Sensor Networks," *Information Fusion, 2007 10th International Conference on* 1.1 (2007): 1-7, 9-12 Web. 2 Jan. 2011.
- [19] Parkka, J., Ermes, M., Antila, K., van Gils, M., Manttari, A., Nieminen, H. "Estimating Intensity of Physical Activity: A Comparison of Wearable Accelerometer and Gyro Sensors and 3 Sensor Locations," *Engineering in Medicine and Biology Society, 2007. EMBS 2007. 29th Annual International Conference of the IEEE* 1.1 (2007): 1511-1514, 22-26 Web. 2 Jan. 2011.
- [20] Tapia, E.M., Intille, S.S., Haskell, W., Larson, K., Wright, J., King, A., Friedman, R. "Real-Time Recognition of Physical Activities and Their Intensities Using Wireless Accelerometers and a Heart Rate Monitor," *Wearable Computers, 2007 11th IEEE International Symposium on* 1.1 (2007): 37-40, 11-13 Web. 2 Jan. 2011.

- [21] Chuo, Y., Marzencki, M., Hung, B., Jaggernaut, C., Tavakolian, K., Lin, P., Kaminska, B. "Mechanically Flexible Wireless Multisensor Platform for Human Physical Activity and Vitals Monitoring," *Biomedical Circuits and Systems, IEEE Transactions on* 4.5 (2010): 281-294 Web. 2 Jan. 2011.
- [22] "Analog Devices ADXL345" Analog Devices. May 2009. Web. 1 Feb. 2011.
- [23] "ITG-3200 Product Specification" InvenSense. March 2010. Web. 28 Jan. 2011.
- [24] "Dual Emitter/ Matching Photodetector Series Datasheet." OSI Optoelectronics. (2010). Web. 1 Sep. 2010.
- [25] Graeme, J. *Photodiode Amplifiers: Op Amp Solutions*. McGraw-Hill Professional, 1996. Web. 26 Feb. 2011.